Numerical renormalization group
part 3

Rok Žitko

Jožef Stefan institute

and

Faculty of Mathematics and Physics, University of Ljubljana, Slovenia

Uberlandia school of advanced studies, January 2019

- Dynamical quantities (spectra)
- Discretization and truncation errors
- Transport properties

Ground state and excited states

$$H|\psi_n\rangle = E_n|\psi_n\rangle$$

thermodynamics:

$$Z = \mathrm{Tr}\left[e^{-\beta H}\right] = \sum_n e^{-\beta E_n} \qquad \beta = \frac{1}{k_B T}$$

dynamics:

$$x(t) = \int_{-\infty}^{t} \chi(t-t')\, h(t')\, \mathrm{d}t$$

$$\chi(t-t') = -i\langle[A(t), B(t')]\rangle$$

Kubo formalism, linear response

Green's functions

$$G_{AB}(t) = \langle\langle A, B\rangle\rangle_t \equiv -i\theta(t)\langle[A(t), B(0)]_\pm\rangle \qquad A(t) = e^{iHt}Ae^{-iHt}$$

$$G_{AB}(z) = \langle\langle A, B\rangle\rangle_z = \int_0^\infty e^{izt}G_{AB}(t)\,dt, \quad \Im z > 0$$

Spectral theorem:

$$\rho_{AB}(\omega) = -\frac{1}{2\pi i}\left(G_{AB}(\omega + i\delta) - G_{AB}(\omega - i\delta)\right) \equiv -\frac{1}{\pi}G''_{AB}(\omega)$$

$$G_{AB}(z) = \int_{-\infty}^{\infty} \frac{\rho_{AB}(\omega)}{z - \omega}d\omega$$

Spectral decomposition

Correlation functions: $C^{>}_{AB} = \langle A(t)B \rangle \qquad C^{<}_{AB} = \langle BA(t) \rangle$

$$C^{>,<}_{AB}(\omega) = \int_{-\infty}^{\infty} e^{i\omega t} C^{>,<}_{AB}(t)$$

$$G_{AB}(t) = -i\theta(t)(C^{>}_{AB}(t) + \epsilon C^{<}_{AB}(t))$$

ε=+1 if A and B are fermionic, otherwise ε=-1.

Spectral representation: $G_{AB}(z) = \int_{-\infty}^{\infty} \mathrm{d}\omega \frac{\rho_{AB}(\omega)}{z - \omega}$

Spectral function: $\rho_{AB}(\omega) = \frac{1}{2\pi} \left(C^{>}_{AB}(\omega) + \varepsilon C^{<}_{AB}(\omega) \right)$

Lehmann representation

$$p_n = e^{-\beta E_n}$$

$$C^{>}_{AB}(t) = \langle e^{iHt} A e^{-iHt} B \rangle = \sum_{nm} p_n A_{nm} B_{mn} e^{i(E_n - E_m)t}$$

$$C^{>}_{AB}(\omega) = \sum_{nm} p_n A_{nm} B_{mn} 2\pi\delta(\omega + E_n - E_m)$$

$$C^{<}_{AB}(\omega) = \sum_{nm} p_m A_{nm} B_{mn} 2\pi\delta(\omega + E_n - E_m)$$

$$G''_{AB}(\omega) = -\pi \sum_{nm} p_n A_{nm} B_{mn} \delta(\omega + E_n - E_m)\left(1 + \epsilon e^{-\beta\omega}\right)$$

$$\rho_{AB}(\omega) = -\frac{1}{\pi} G''_{AB}(\omega)$$

Lehmann representation for impurity spectral function

$$A(\omega) = \sum_{nm} \left| \langle m | d^\dagger | n \rangle \right|^2 \delta(\omega - E_m - E_n) \frac{e^{-\beta E_m} + e^{-\beta E_n}}{Z}$$

T=0 vs. T≠0

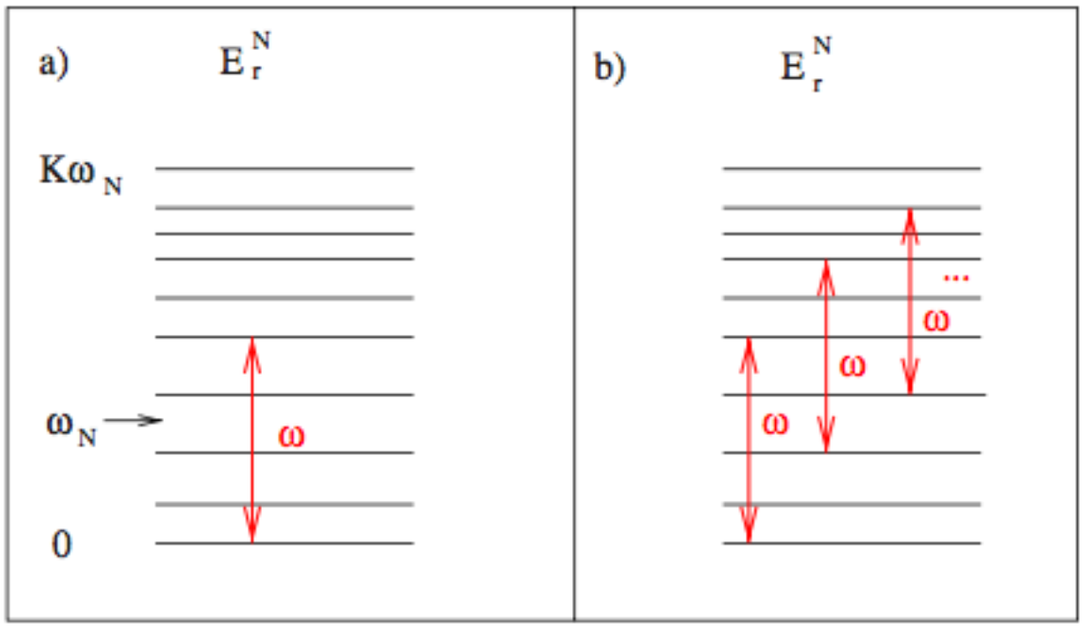

FIG. 9. (Color online) Excitations of H_N contributing to the spectral function at frequency ω for (a) $T=0$ and (b) $T>0$.

Simplest approach

Traditional way: at NRG step N we take excitation energies in the interval [$a\ \omega_N$: $a\ \Lambda^{1/2}\ \omega_N$] or [$a\ \omega_N$: $a\ \Lambda\ \omega_N$], where a is a number of order 1. This defines the value of the spectral function in this same interval.

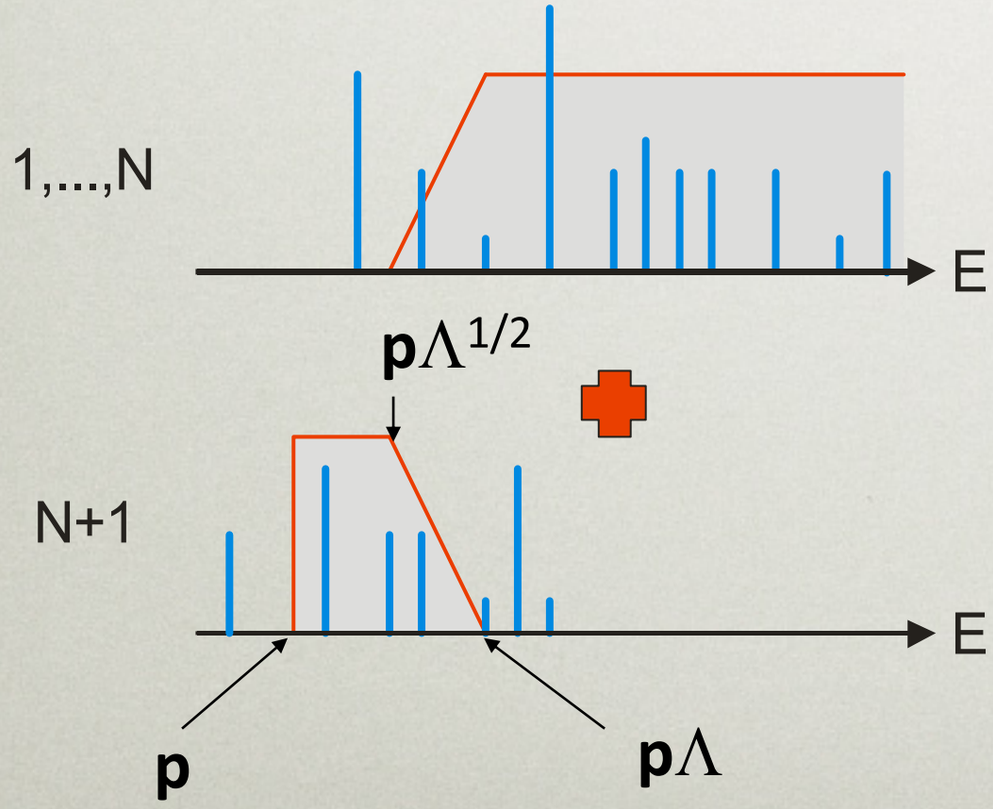

"patching"

p: patching parameter (in units of energy scale at N+1-th iteration)

Broadening

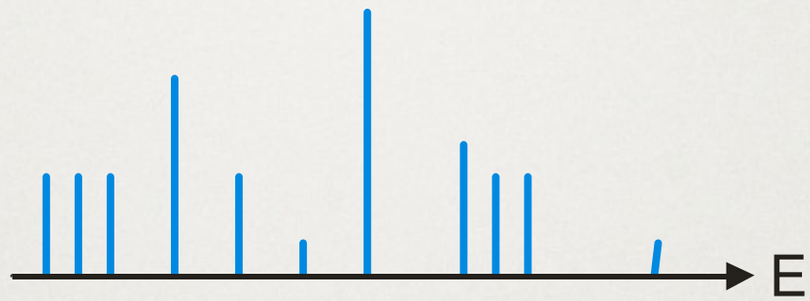

Traditional log-Gaussian

$$lG(\omega, E) = \frac{e^{-b^2/4}}{bE\sqrt{\pi}} \exp\left[-\left(\frac{(\log\omega - \log E}{b}\right)^2\right]$$

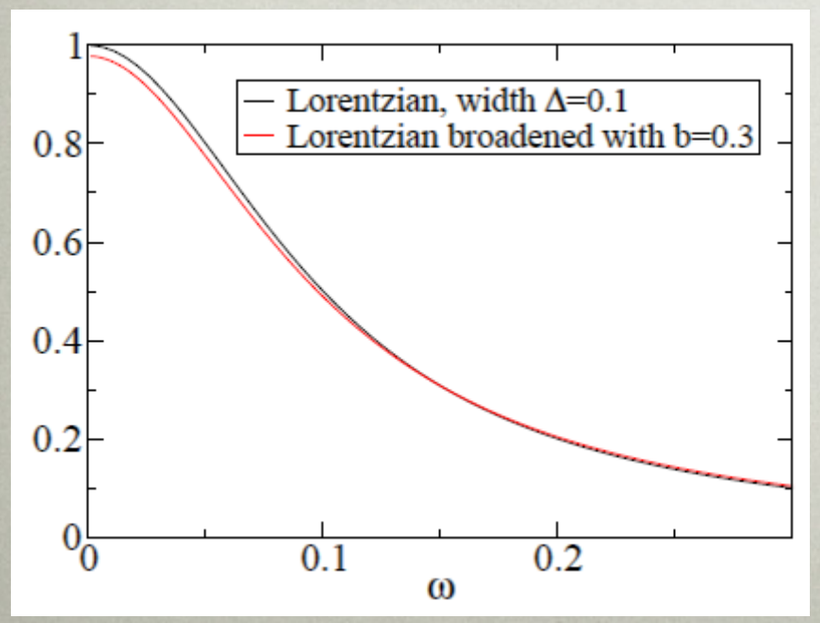

$$\delta\omega_+ = \omega\left(e^{b\sqrt{\ln 2}} - 1\right)$$
$$\delta\omega_- = \omega\left(1 - e^{-b\sqrt{\ln 2}}\right)$$

MODIFIED LOG-GAUSSIAN

$$mLG(\omega, E) = \frac{1}{\alpha|\omega|\sqrt{\pi}} \exp\left[-\left(\frac{\log(\omega/E)}{\alpha} - \frac{\alpha}{4}\right)^2\right]$$

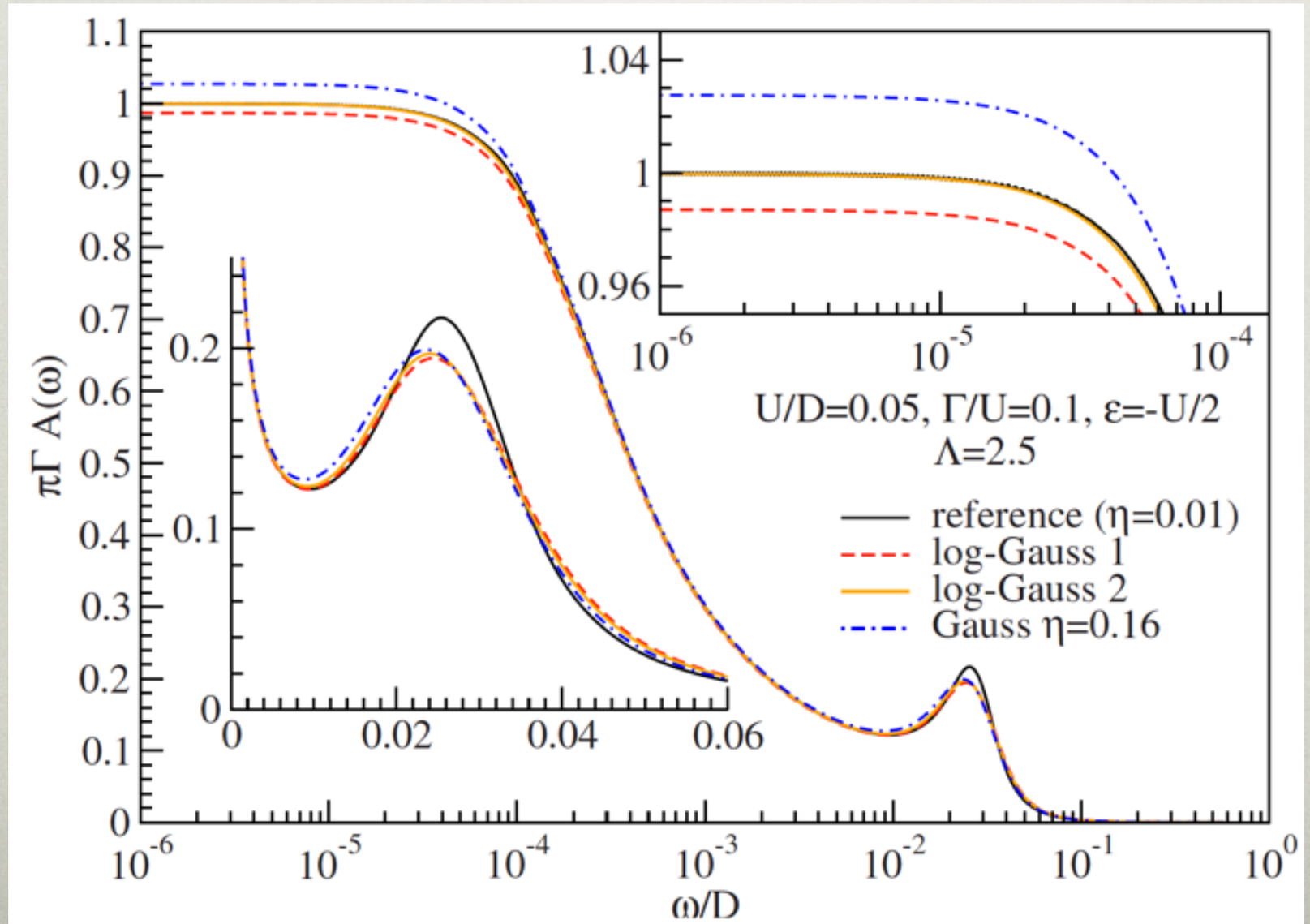

Broadening at finite temperatures

Second stage of broadening:

$$G(\omega, E) = \frac{1}{\omega_0 \sqrt{\pi}} \exp\left[- \left(\frac{\omega - E}{\omega_0} \right)^2 \right]$$

$$\omega_0 \propto T$$

```
[extra]
U=0.01
Gamma=0.001
delta=0

[param]
symtype=QS
discretization=Z
Lambda=2
Tmin=1e-10
keepenergy=10
keep=5000

model=SIAM
```

```
ops=A_d
specd=A_d-A_d
```

choice of operators / spectra

A_d $\langle m|d_\sigma^\dagger|n\rangle$

A_d-A_d $\langle\langle d_\sigma; d_\sigma^\dagger\rangle\rangle_\omega$

```
broaden_max=0.1
broaden_min=1e-7
broaden_ratio=1.02
```

frequency mesh for output

$$\omega_n = \text{broaden\_max} \times \text{broaden\_ratio}^{-n}$$

```
fdm=true
T=1e-10
```

algorithm

```
smooth=new
alpha=0.6
omega0=1e-99
```

spectral smoothing

$$\rho_{AB}(\omega) = -\frac{1}{\pi}\mathrm{Im}\left[\langle\langle A^\dagger; B\rangle\rangle_\omega\right]$$

`spec_FDM_dens_A_d-A_d.dat`

This is the spectral function = imaginary part of the Green's function.
Real part can be obtained using the Kramers-Kronig transformation.

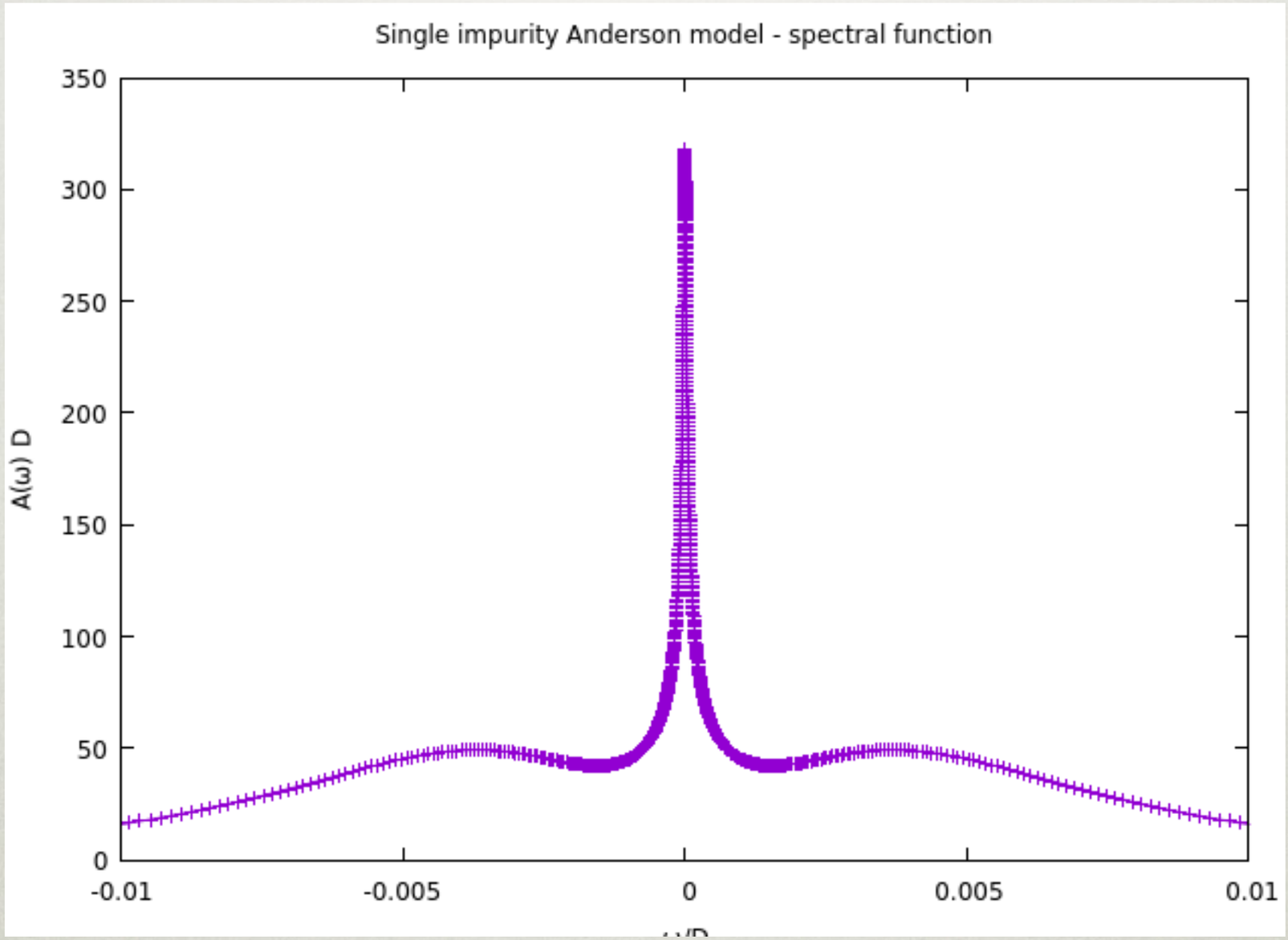
Single impurity Anderson model - spectral function
A(ω) D
350
300
250
200
150
100
50
0
-0.01
-0.005
0
0.005
0.01

Friedel sum rule

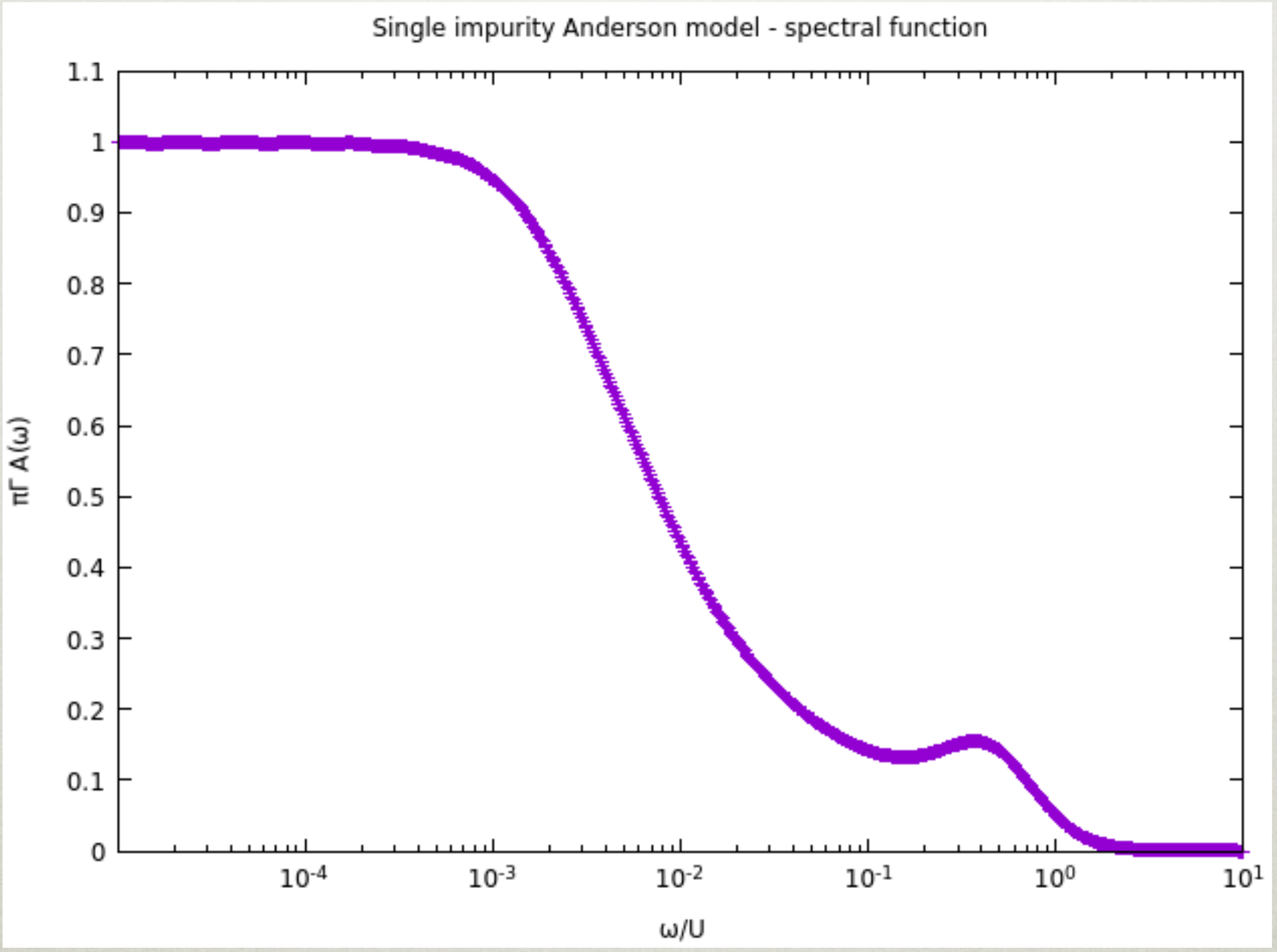

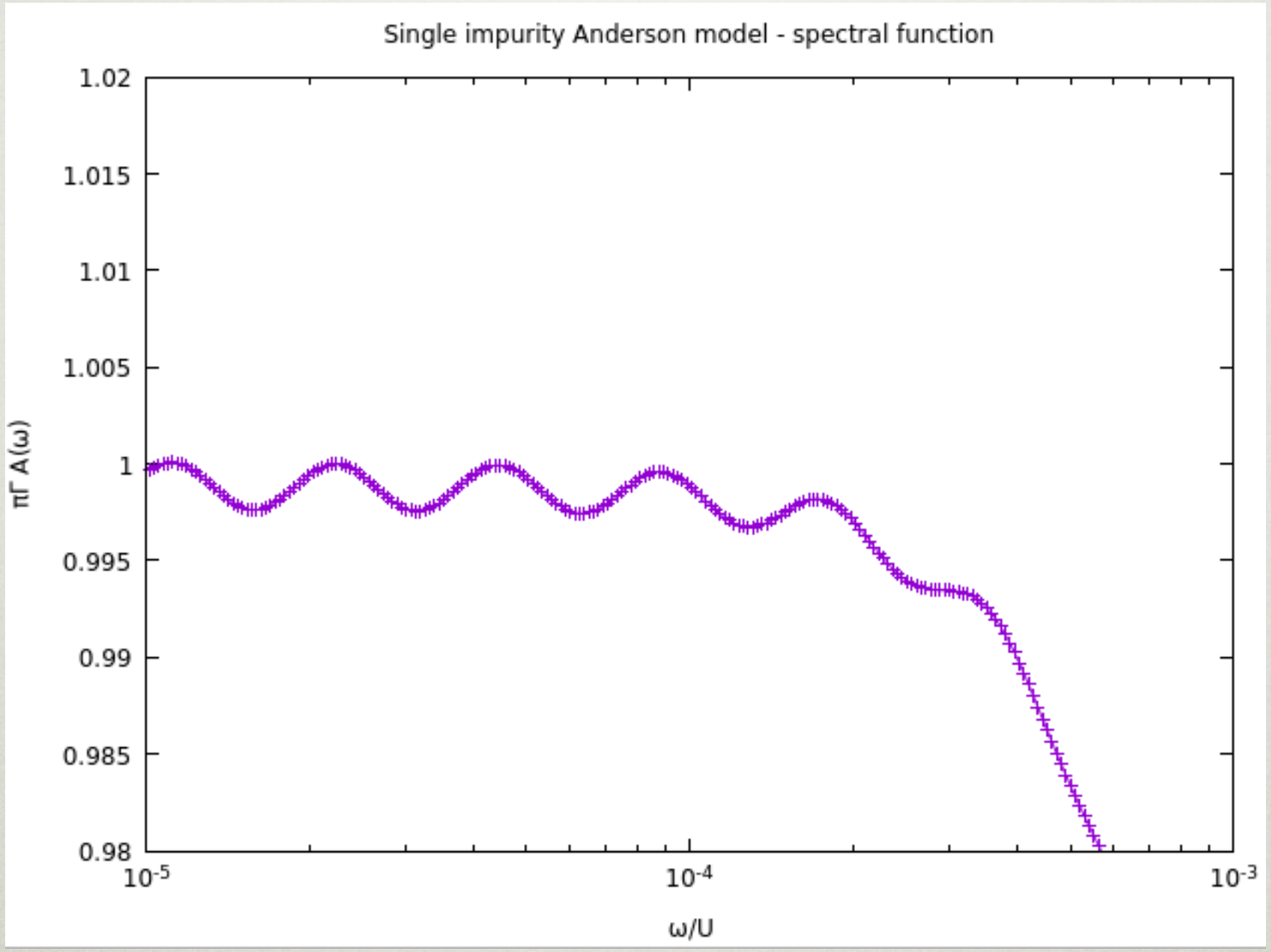
Single impurity Anderson model - spectral function
πΓ A(ω)
1.02
1.015
1.01
1.005
1
0.995
0.99
0.985
0.98
10-5
10-4
10-3
ω/U

Density-matrix NRG

Problem: Higher-energy parts of the spectra calculated without knowing the true ground state of the system

Solution:

1) Compute the density matrix at the temperature of interest. It contains full information about the ground state.
2) Evaluate the spectral function in an additional NRG run using the *reduced density matrix* instead of the simple Boltzmann weights.

$$T = 0 \quad \rightarrow \quad \rho = |0\rangle\langle 0|$$

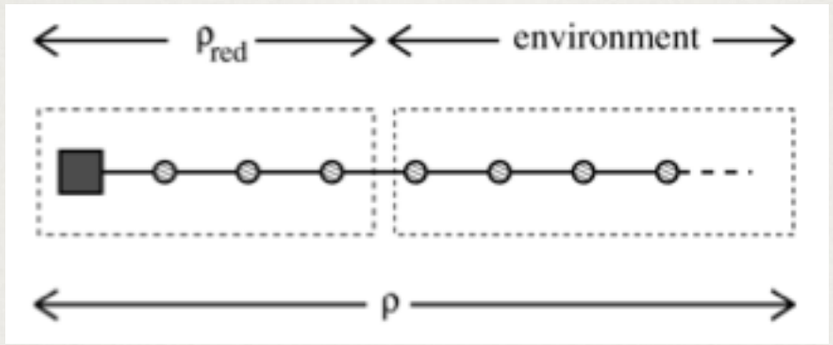

$$\hat{\rho} = \sum_{m_1,m_2,n_1,n_2} \rho_{m_1 n_1 m_2 n_2} |m_1\rangle_{\mathrm{env}} |n_1\rangle_{\mathrm{sys}} \langle n_2| \langle m_2|$$

$$\hat{\rho}^{\mathrm{red}} = \sum_{n_1,n_2} \rho^{\mathrm{red}}_{n_1 n_2} |n_1\rangle_{\mathrm{sys}} \langle n_2| \qquad \rho^{\mathrm{red}}_{n_1 n_2} = \sum_m \rho_{m n_1, m n_2}$$

W. Hofstetter, PRL 2000

DMNRG for non-Abelian symmetries: Zitko, Bonca, PRB 2006

Spectral function computed as:

$$A_\mu^N(\omega) = \sum_{ijm} \left(\langle j|d_\mu^\dagger|m\rangle\langle j|d_\mu^\dagger|i\rangle \rho_{im}^{\text{reduced}} + \langle j|d_\mu^\dagger|m\rangle\langle i|d_\mu^\dagger|m\rangle \rho_{ji}^{\text{reduced}} \right) \delta(\omega - (E_j - E_m))$$

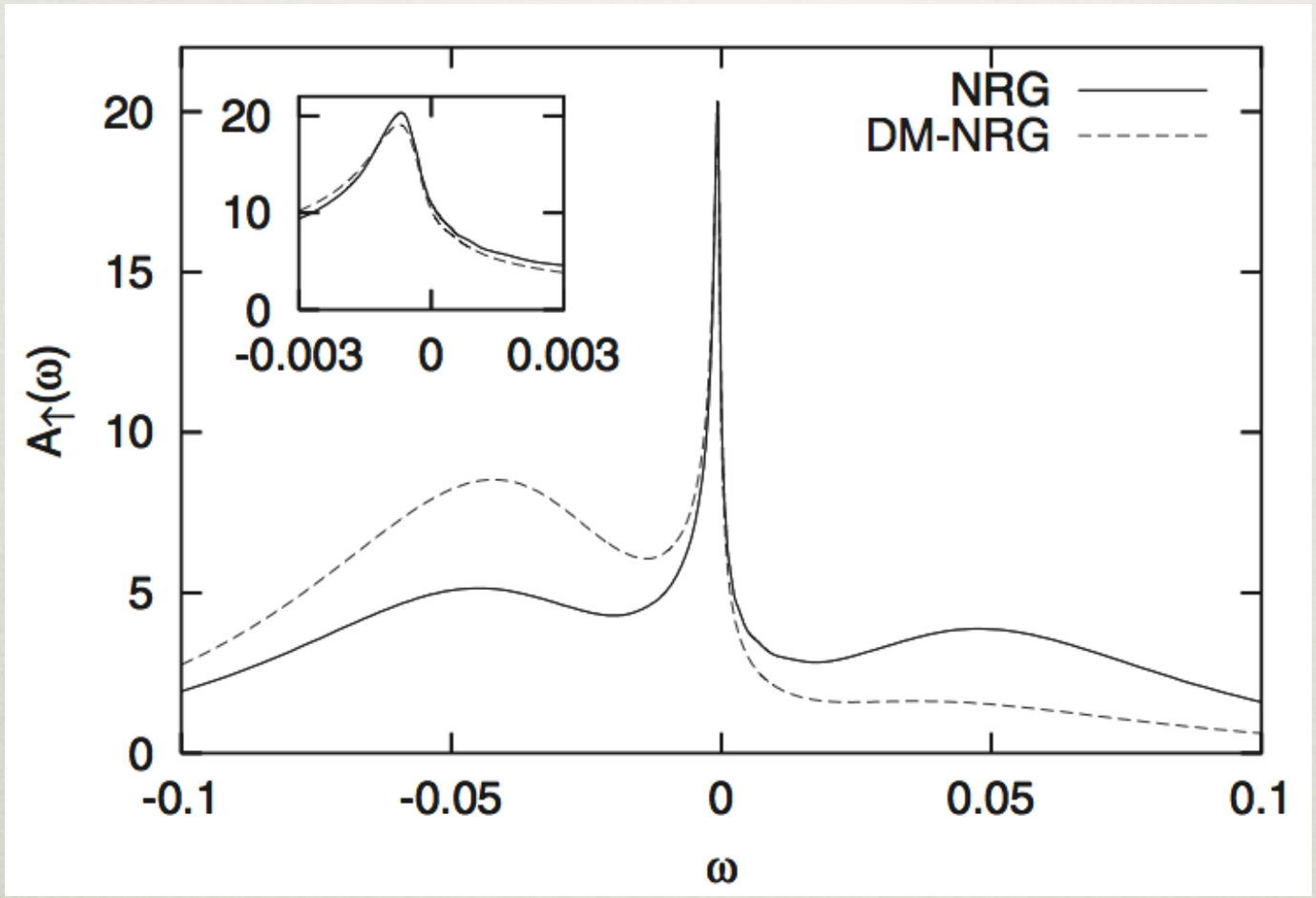

W. Hofstetter, PRL 2000

CFS & FDM-NRG

CFS = complete Fock space
FDM = full density matrix

Anders, Schiller, PRL 2005, PRB 2006

Peters, Pruschke, Anders, PRB 2006

Weichselbam, von Dellt, PRL 2007

COMPLETE BASIS SET FOR WILSON CHAIN

$$|\alpha_{\rm imp}, \alpha_0, \ldots, \alpha_N\rangle$$

m: shell label

$$|r, e; m\rangle \qquad e = \{\alpha_{m+1}, \ldots, \alpha_N\}$$

$$|k, e; m\rangle_{\rm kp} \qquad |l, e; m\rangle_{\rm dis}$$

$$\mathcal{F}_N = {\rm span}\{|l, e; m\rangle_{\rm dis}\}$$

Anders, Schiller, PRL 2005, PRB 2006

$$\rho = \sum_m \sum_{le} |le; m\rangle \frac{e^{-\beta E_l^m}}{Z} \langle le; m|$$

Weichselbam, von Dellt, PRL 2007

$$\sum_{m=m_{\min}}^{N} \sum_{l,e} |l,e;m\rangle_{\mathrm{dis}\ \ \mathrm{dis}}\langle l,e;m| = 1$$

$$1_m^- = \sum_{m'=m_{\min}}^{m} \sum_{l',e'} |l',e';m'\rangle_{\mathrm{dis}\ \ \mathrm{dis}}\langle l',e';m'|,$$

$$1_m^+ = \sum_{m'=m+1}^{N} \sum_{l',e'} |l',e';m'\rangle_{\mathrm{dis}\ \ \mathrm{dis}}\langle l',e';m'|.$$

$$1_m^+ = \sum_{k,e} |k,e;m\rangle_{kp\ \ kp}\langle k,e;m|$$

Also the basis of the time-dependent NRG !
(cf. Anders, Schiller 2005, 2006)

$$\mathrm{Tr}[\hat{\rho}e^{iHt}Ae^{-iHt}B] = \sum_{l,e,m}\sum_{l',e',m'} \mathrm{Tr}[\hat{\rho}e^{iHt}|l,e;m\rangle\langle l,e;m|Ae^{-iHt}|l',e';m'\rangle\langle l',e';m'|B]$$

$$= \sum_{m}\sum_{l,e}\sum_{l',e'} {}_{\mathrm{dis}}\langle l,e;m|Ae^{-iHt}|l',e';m\rangle_{\mathrm{dis}}\ {}_{\mathrm{dis}}\langle l',e';m|B\hat{\rho}e^{iHt}|l,e;m\rangle_{\mathrm{dis}}$$

$$+ \sum_{m}\sum_{l,e}\sum_{k,e'} {}_{\mathrm{dis}}\langle l,e;m|Ae^{-iHt}|k,e';m\rangle_{kp}\ {}_{kp}\langle k,e';m|B\hat{\rho}e^{iHt}|l,e;m\rangle_{\mathrm{dis}}$$

$$+ \sum_{m}\sum_{l,e'}\sum_{k,e} {}_{\mathrm{dis}}\langle l,e';m|B\hat{\rho}e^{iHt}|k,e;m\rangle_{kp}\ {}_{kp}\langle k,e;m|Ae^{-iHt}|l,e';m\rangle_{\mathrm{dis}}.$$

Peters, Pruschke, Anders 2006

$$G^{i}_{A,B}(z) = \frac{1}{Z}\sum_{l,l'} \langle l;N|A|l';N\rangle\langle l';N|B|l;N\rangle \frac{e^{-\beta E^N_l} - s e^{-\beta E^N_{l'}}}{z + E^N_l - E^N_{l'}}.$$

$$G^{ii}_{A,B}(z) = \sum_{m=m_{\min}}^{N-1} \sum_{l} \sum_{k,k'} A_{l,k'}(m)\rho^{\mathrm{red}}_{k',k}(m)B_{k,l}(m)\frac{-s}{z + E_l - E_k}$$

$$G^{iii}_{A,B}(z) = \sum_{m=m_{\min}}^{N-1} \sum_{l} \sum_{k,k'} B_{l,k'}(m)\rho^{\mathrm{red}}_{k',k}(m)A_{k,l}(m)\frac{1}{z + E_k - E_l},$$

note: s=-1 for fermions

Peters, Pruschke, Anders 2006

CFS vs FDM vs DMNRG

- CFS and FDM equivalent at T=0
- FDM recommended at T>0
- CFS and FDM are slower than DMNRG
  (all states need to be determined, more complex expressions for spectral functions)
- No patching, thus no arbitrary parameter as in DMNRG

param

```
finite=true
dmnrg=true
fdm=true
cfs=true
```

Self-energy trick

$$G_\sigma(\omega) = \langle\langle d_\sigma; d_\sigma^\dagger \rangle\rangle_\omega$$

A=-1/π Im[G]

$$F_\sigma(\omega) = \langle\langle n_{-\sigma} d_\sigma; d_\sigma^\dagger \rangle\rangle_\omega$$

B=-1/π Im[F]

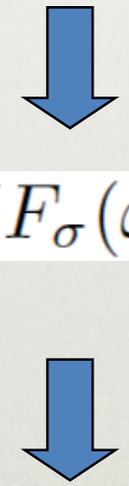

$$\Sigma_\sigma(\omega) = U F_\sigma(\omega)/G_\sigma(\omega)$$

$$G_\sigma^{\text{improved}}(\omega) = \frac{1}{\omega - \epsilon - \Sigma(\omega) + \Delta(\omega)}$$

Bulla, Hewson, Pruschke 1998

param

```
ops=A_d self_d
specd=A_d-A_d self_d-A_d
```

model.m

```
(* All operators which contain d[], except hybridization (Hc). *)
Hselfd = H1;

selfopd = ( Chop @ Expand @ komutator[Hselfd /. params, d[#1, #2]] )&;

(* Evaluate *)
Print["selfopd[CR,UP]=", selfopd[CR, UP]];
Print["selfopd[CR,DO]=", selfopd[CR, DO]];
Print["selfopd[AN,UP]=", selfopd[AN, UP]];
Print["selfopd[AN,DO]=", selfopd[AN, DO]];
```

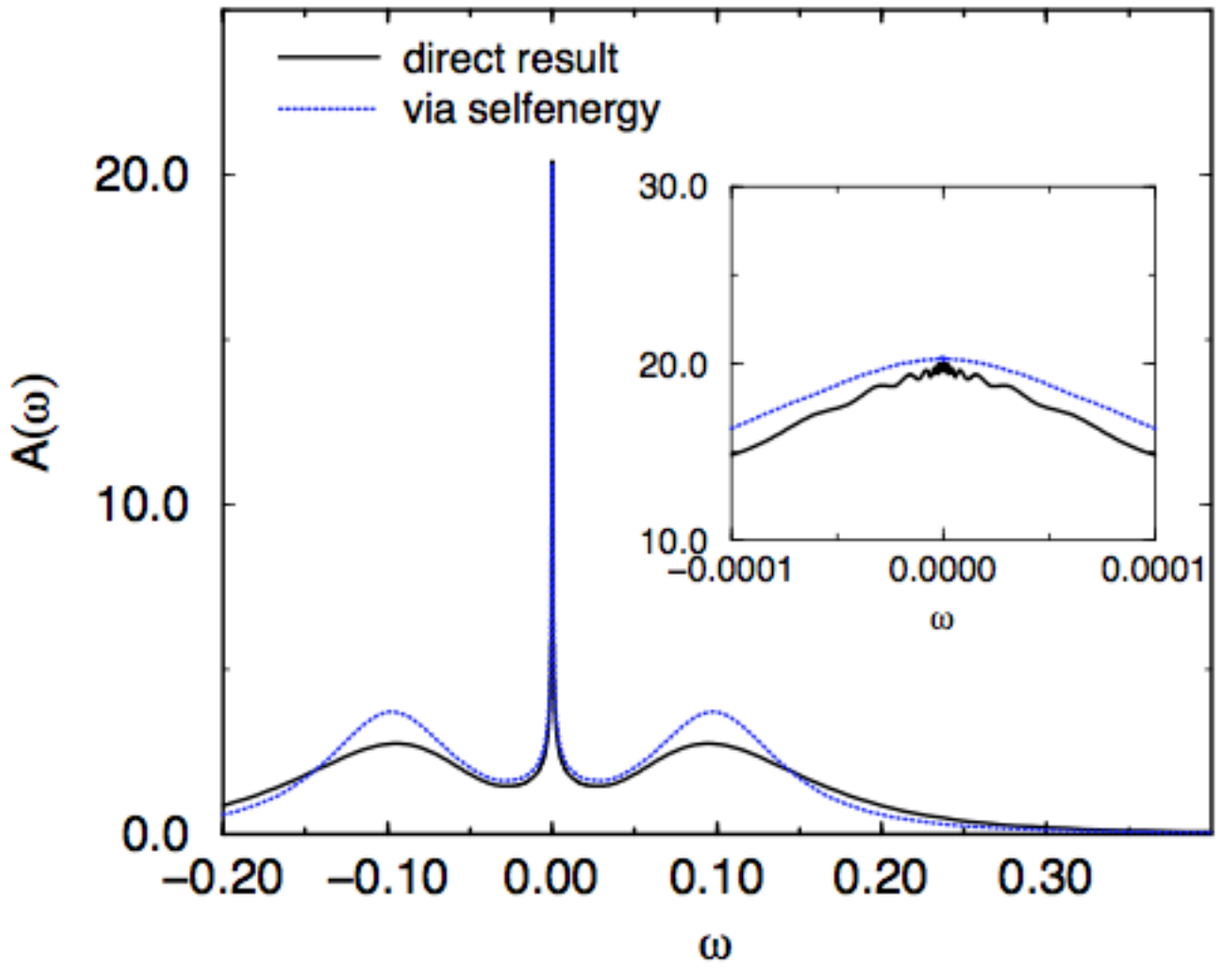

Figure 1. The impurity spectral function for $\varepsilon_f = -0.1, U = 0.2, T = 0$ and $-\mathrm{Im}\,\Delta(\omega+\mathrm{i}0^+) = 0.015$ in units of the conduction electron bandwidth. $\bar{A}(\omega)$ (solid line) is the result obtained directly from the NRG method and $A(\omega)$ (dashed line) is calculated via the self-energy equation (8). The inset shows the region around the Fermi level.

(i) We find for the total spectral weight

$$\int \mathrm{d}\omega\ \bar{A}(\omega) = \bar{w} = 0.93 \qquad \text{and} \qquad \int \mathrm{d}\omega\ A(\omega) = w = 0.9993.$$

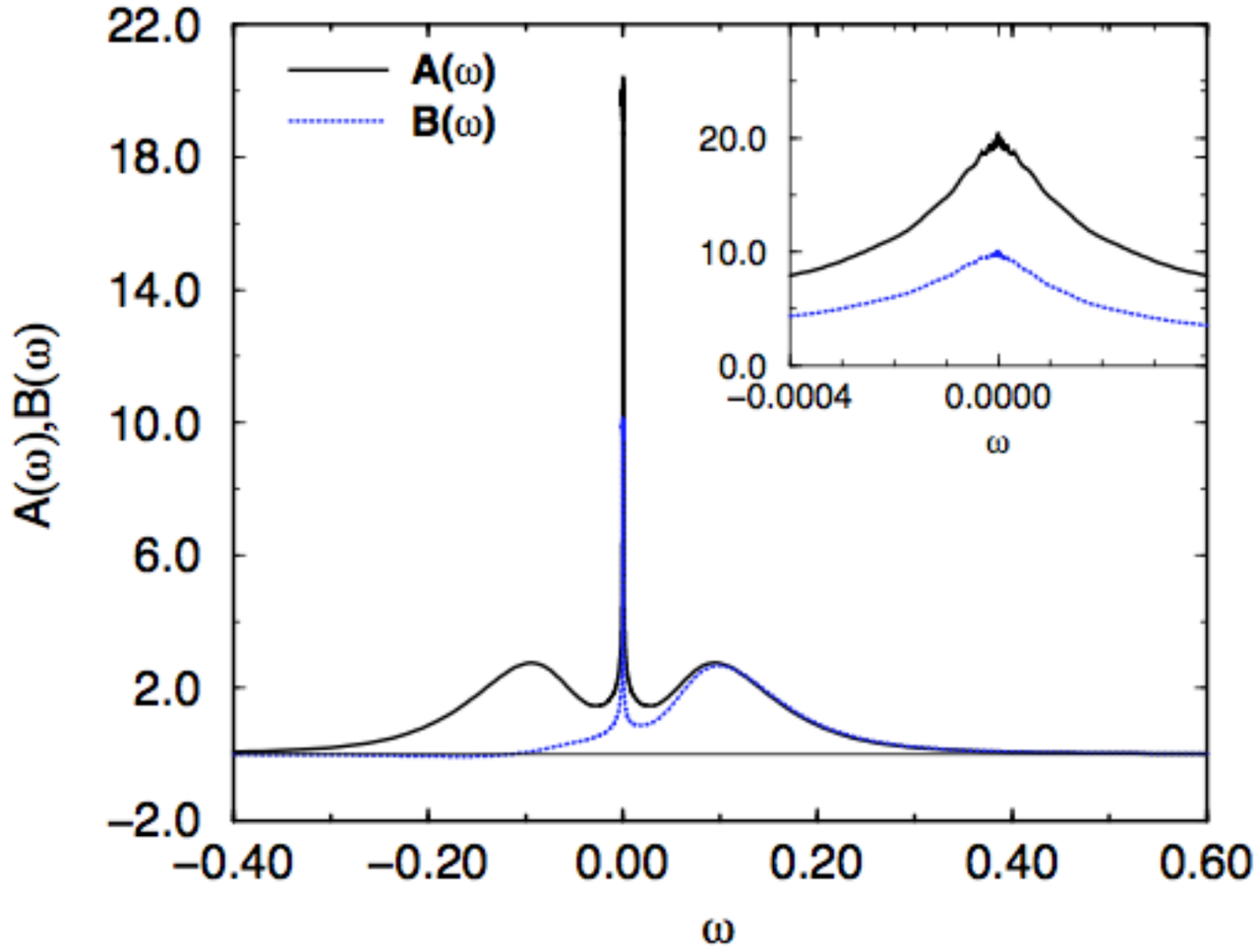

Figure 2. The spectral functions $A(\omega)$ (solid line) and $B(\omega)$ (dotted line) for the same parameters as in figure 1 (directly from the NRG method, not via the self-energy). The inset shows the region around the Fermi level.

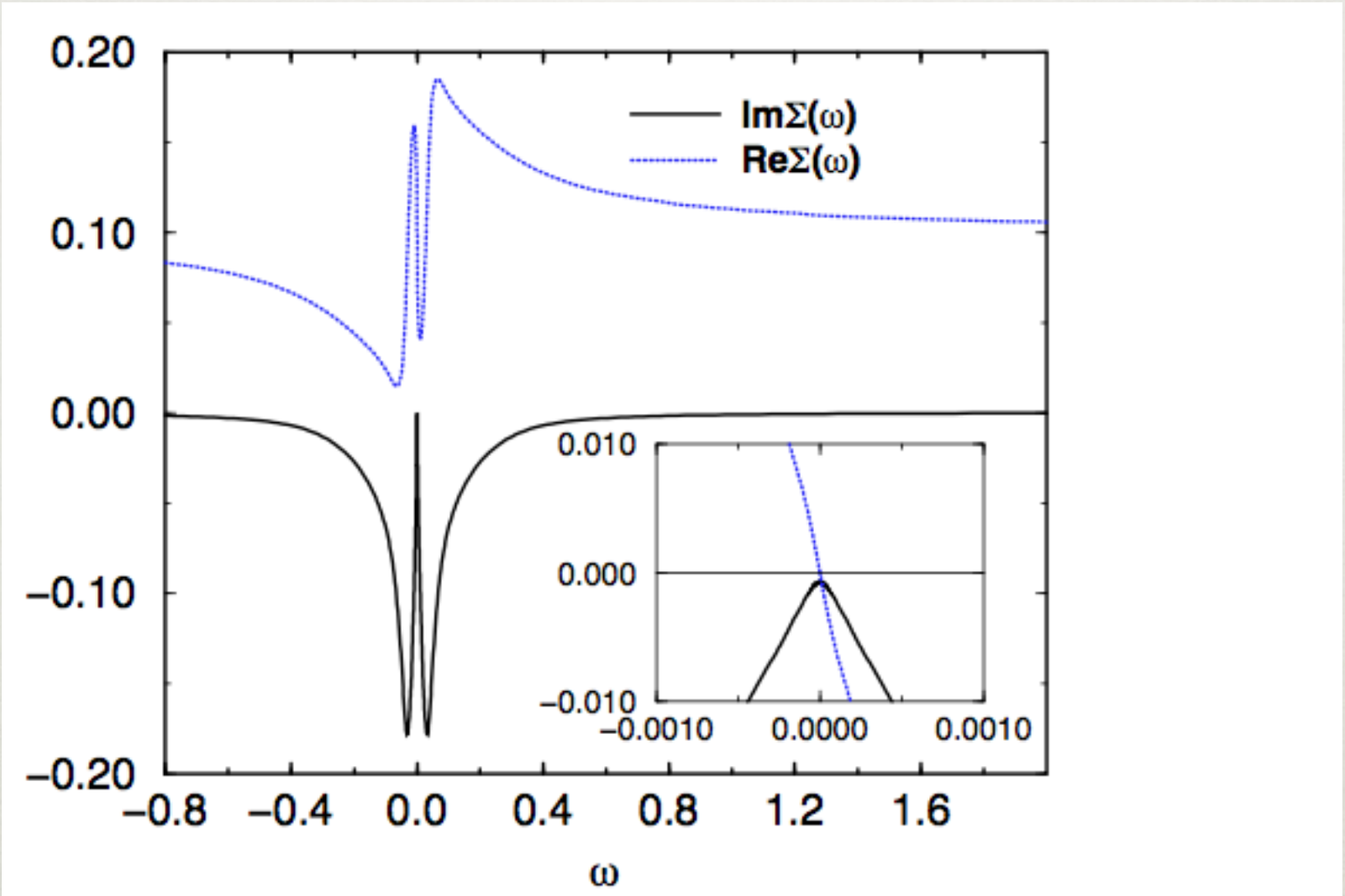

Figure 3. Real and imaginary parts of the self-energy for $\varepsilon_f = -0.1$, $U = 0.2$ and a constant $\Delta_0 = 0.015$. The inset shows the region around the Fermi level where the Hartree term was subtracted from the real part.

In the case of the standard single-impurity Anderson model, we furthermore know that the Friedel sum rule $\mathrm{Im}\,\Sigma^U(\mathrm{i}0^+) = 0$ has to be fulfilled, which implies that

$$\mathrm{Re}\,F(\mathrm{i}0^+) = -\int_{-\infty}^{\infty} \mathrm{d}\omega\; B(\omega)\,\mathcal{P}\frac{1}{\omega} = 0 \tag{15}$$

where $\mathcal{P}(\cdots)$ denotes the principal value. Relation (15) is obviously not trivial as regards the unusual shape of $B(\omega)$. Indeed, it turns out that $\mathrm{Re}\,F(\mathrm{i}0^+)$ is numerically zero as long as the *full* spectrum of the Hamiltonian can be used. However, as soon as a truncation of states sets in, the calculated value for $\mathrm{Re}\,F(\mathrm{i}0^+)$ suddenly jumps to a finite value, eventually leading to a violation of the Friedel sum rule as observed e.g. in figure 1.

This observation suggests that high-energy states are also important to guarantee that $\mathrm{Re}\,F(\mathrm{i}0^+) = 0$ and also that a slight violation of the Friedel sum rule is almost unavoidable in this method.

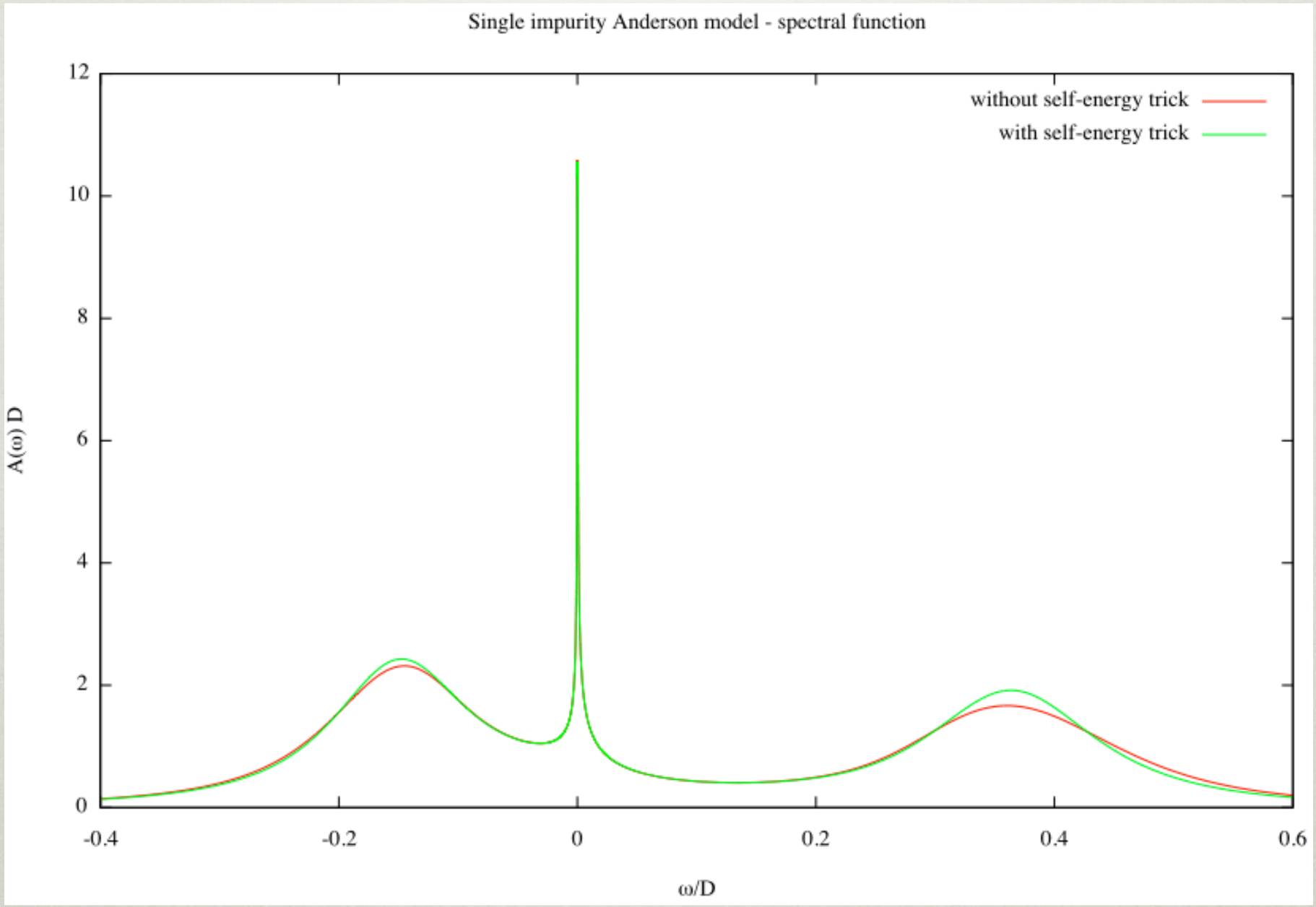
Single impurity Anderson model - spectral function
without self-energy trick
with self-energy trick
A(ω) D
ω/D
12
10
8
6
4
2
0
-0.4
-0.2
0
0.2
0.4
0.6

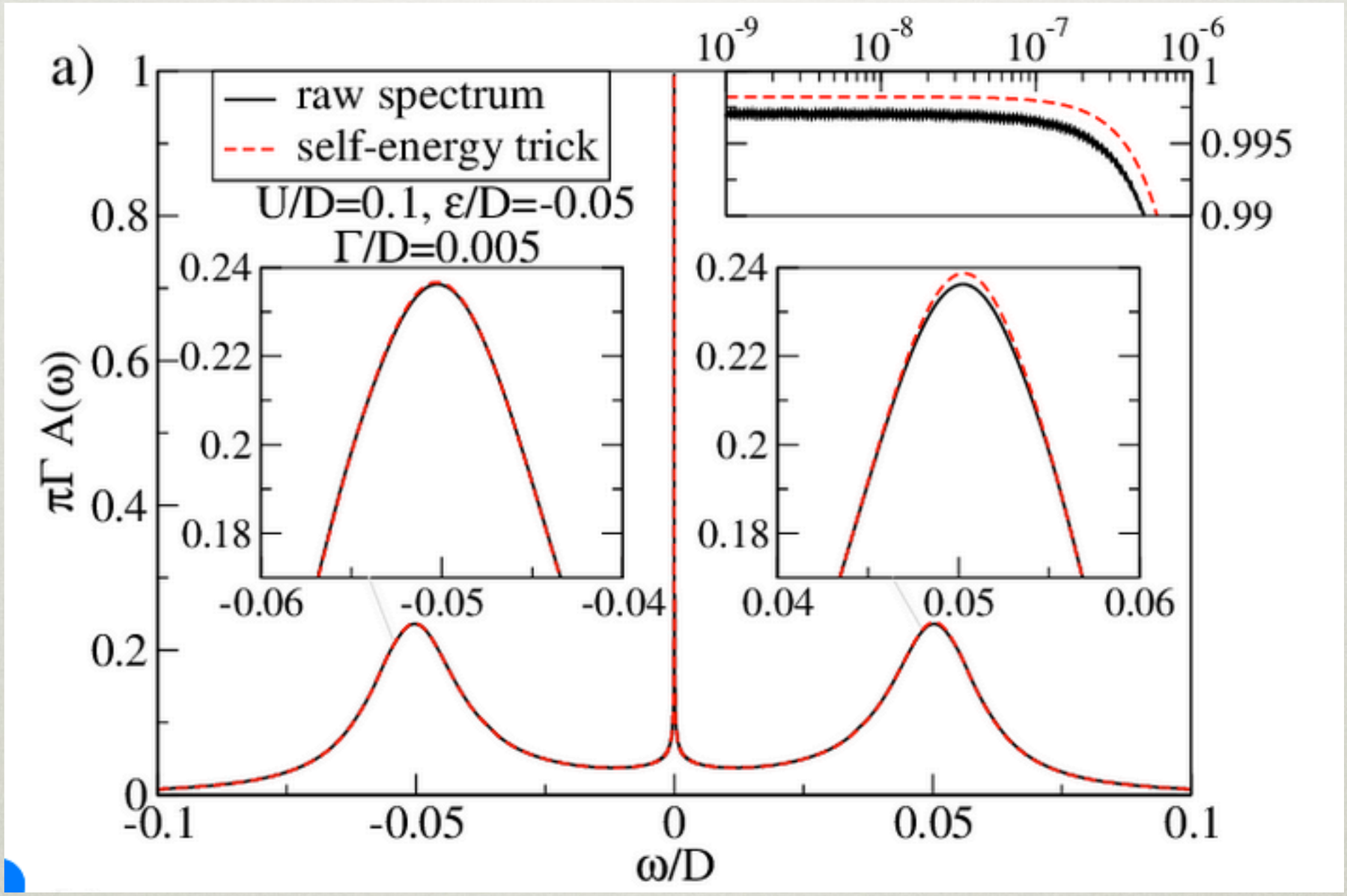
a)
raw spectrum
self-energy trick
U/D=0.1, ε/D=-0.05
Γ/D=0.005
πΓ A(ω)
ω/D
1
0.8
0.6
0.4
0.2
0
-0.1
-0.05
0
0.05
0.1
10^-9
10^-8
10^-7
10^-6
0.995
0.99
0.24
0.22
0.2
0.18
-0.06
-0.05
-0.04
0.04
0.05
0.06

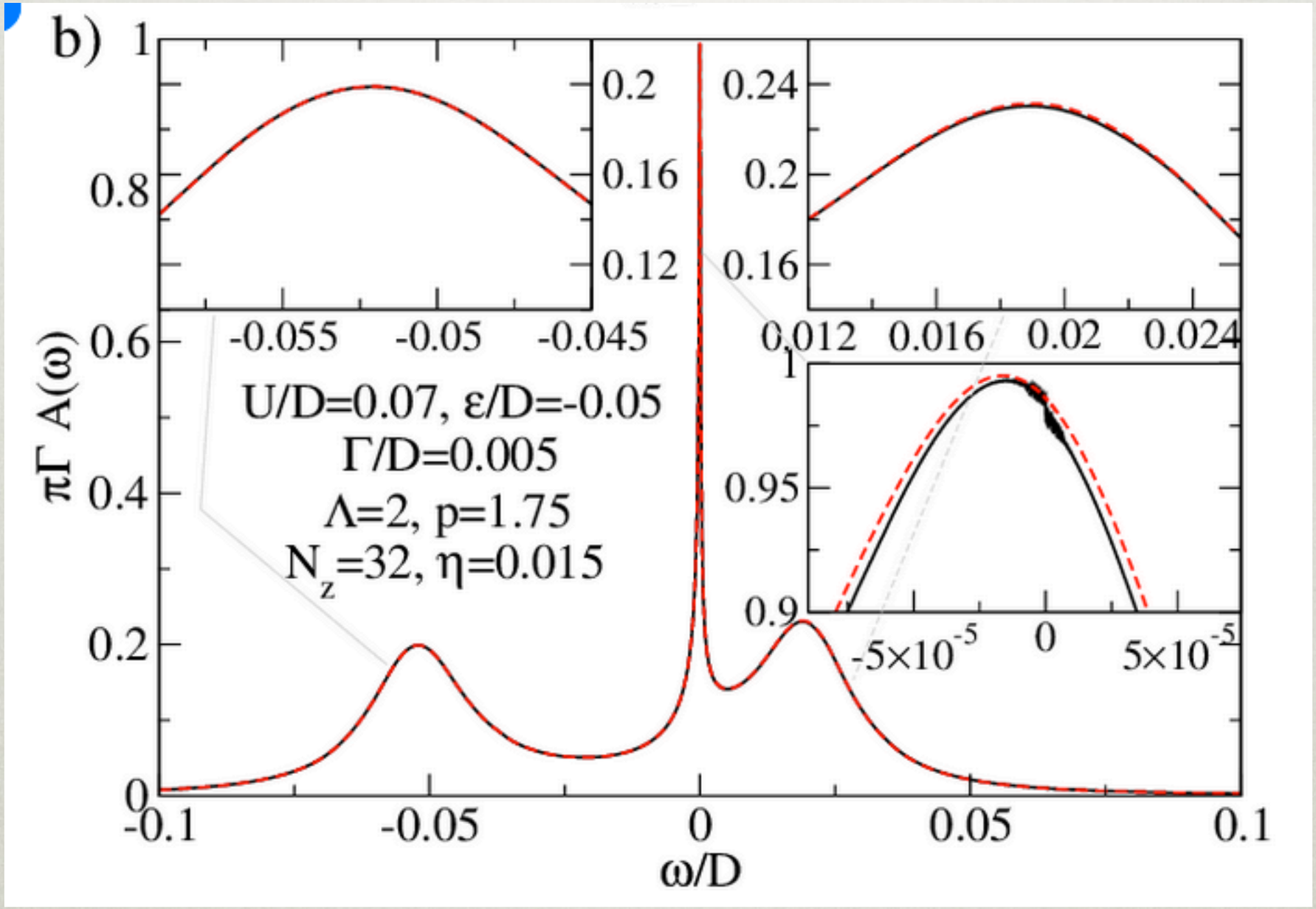
b)
A(ω)
πΓ
U/D=0.07, ε/D=-0.05
Γ/D=0.005
Λ=2, p=1.75
N_z=32, η=0.015
ω/D
-0.1
-0.05
0
0.05
0.1
0
0.2
0.4
0.6
0.8
1
-0.055
-0.05
-0.045
0.12
0.16
0.2
0.012
0.016
0.02
0.024
0.16
0.2
0.24
0.9
0.95
1
-5×10^-5
0
5×10^-5

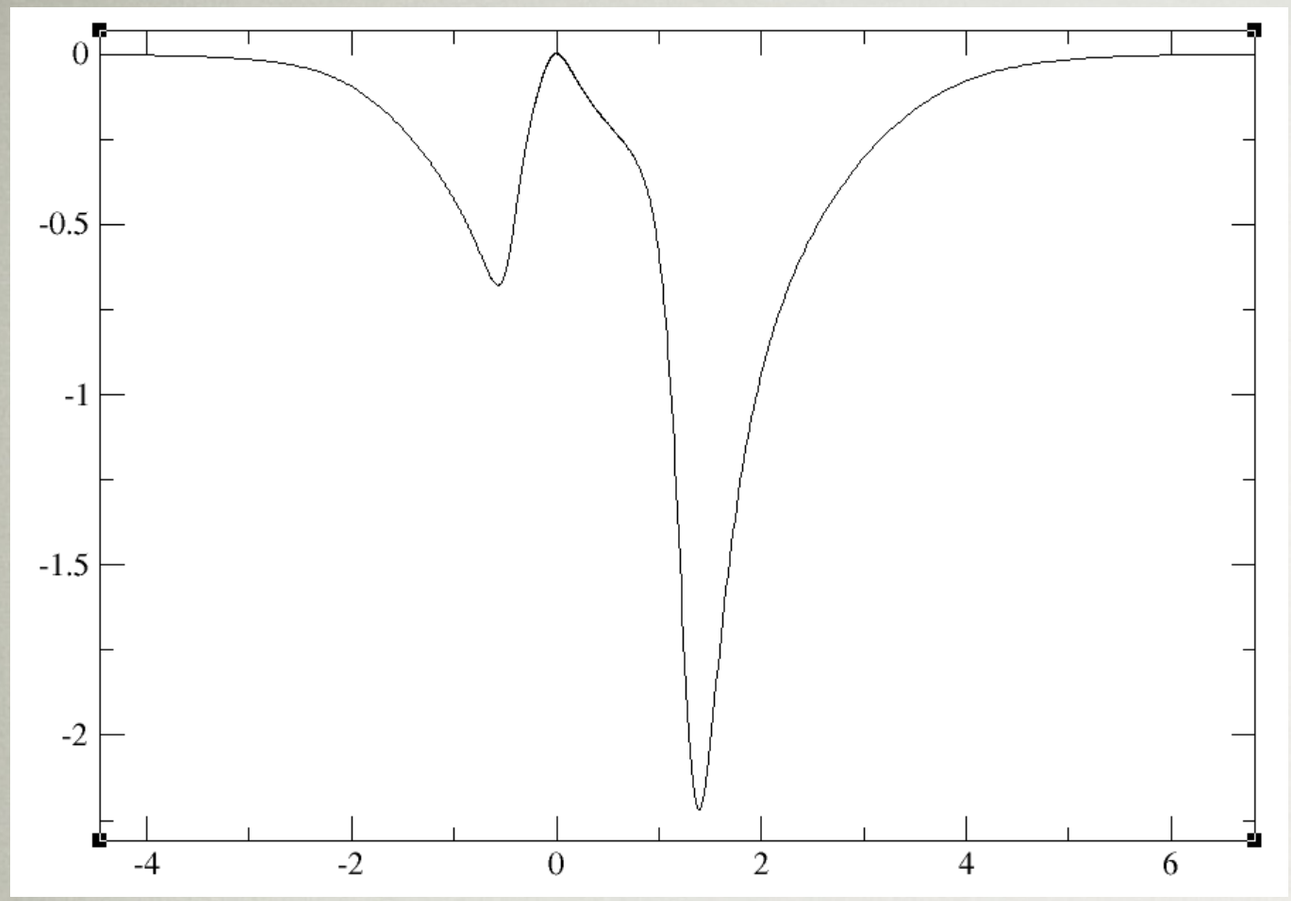
0
-0.5
-1
-1.5
-2
-4
-2
0
2
4
6

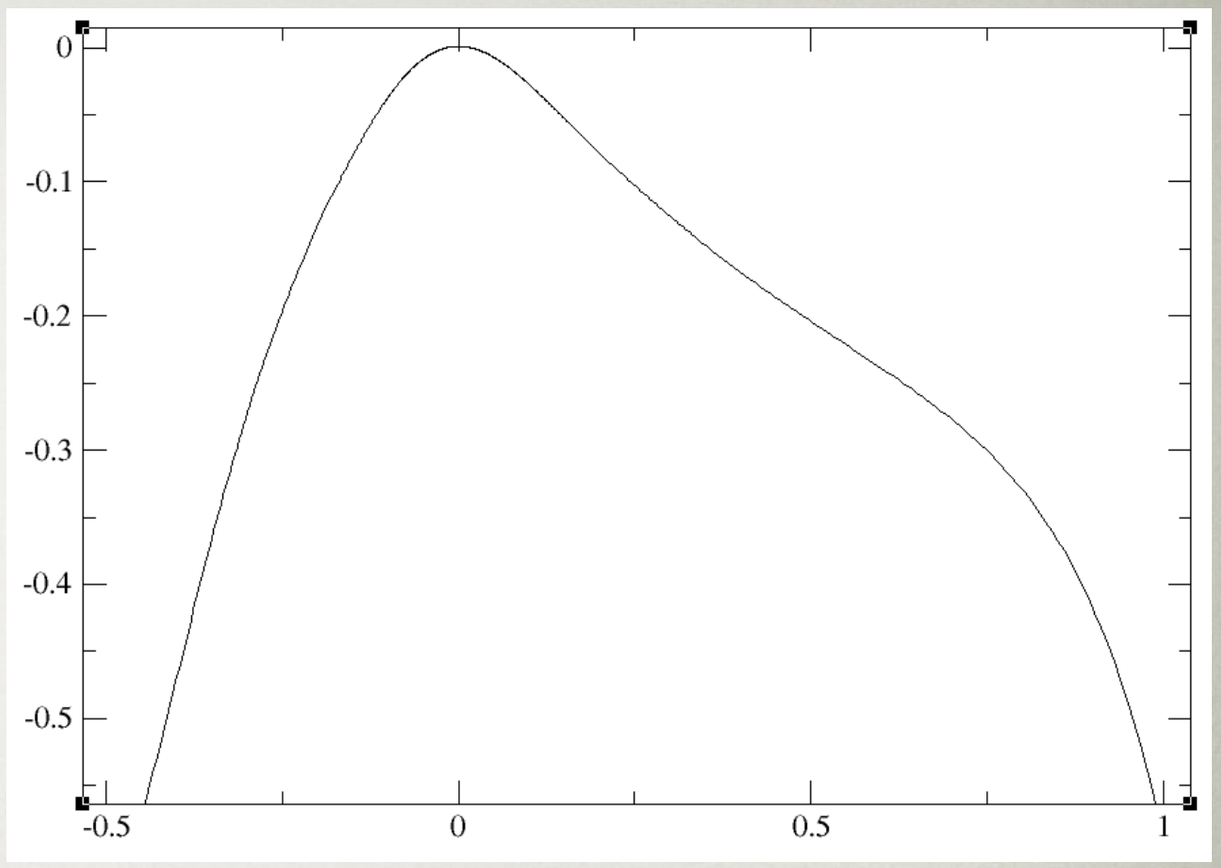
0
-0.1
-0.2
-0.3
-0.4
-0.5
-0.5
0
0.5
1

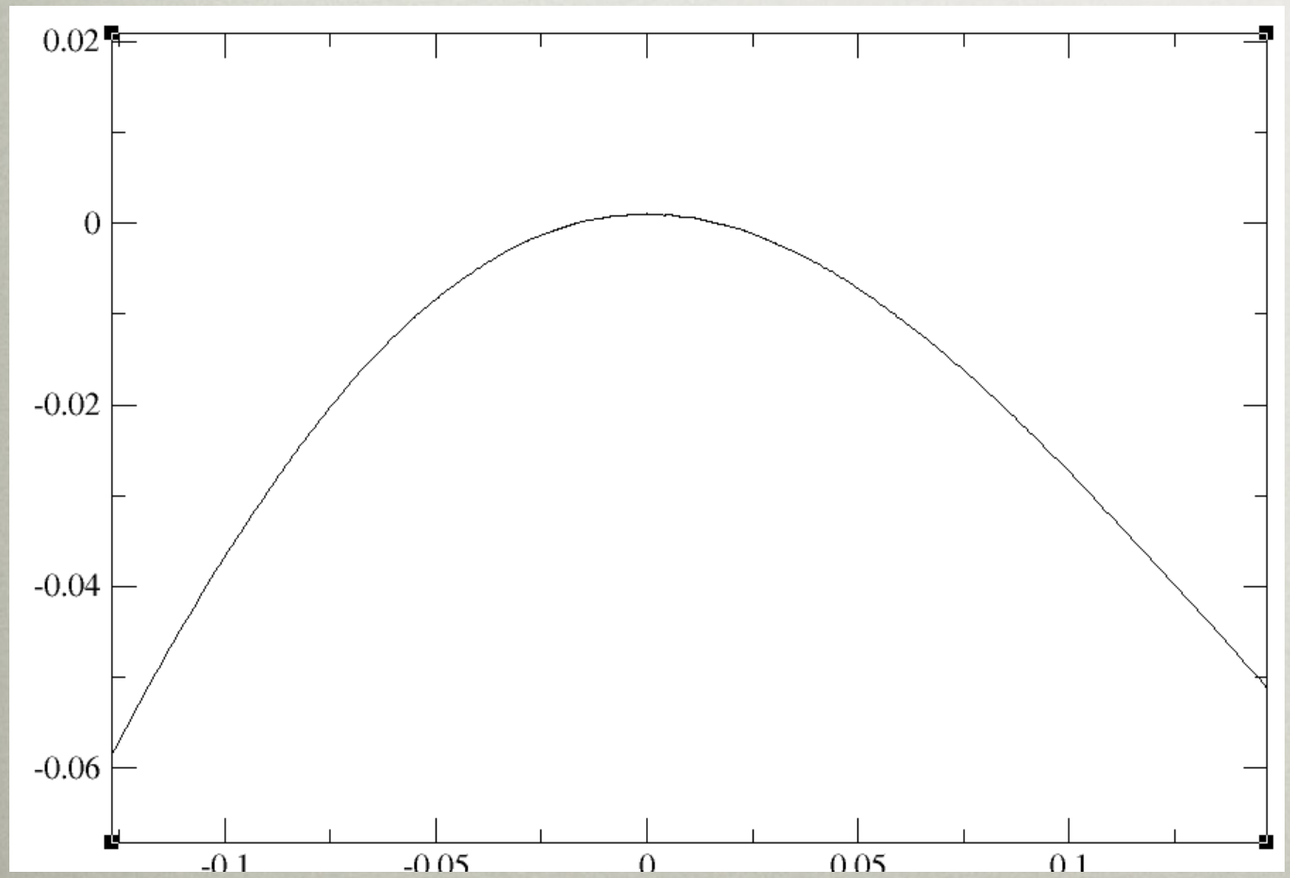
0.02
0
-0.02
-0.04
-0.06
-0.1
-0.05
0
0.05
0.1

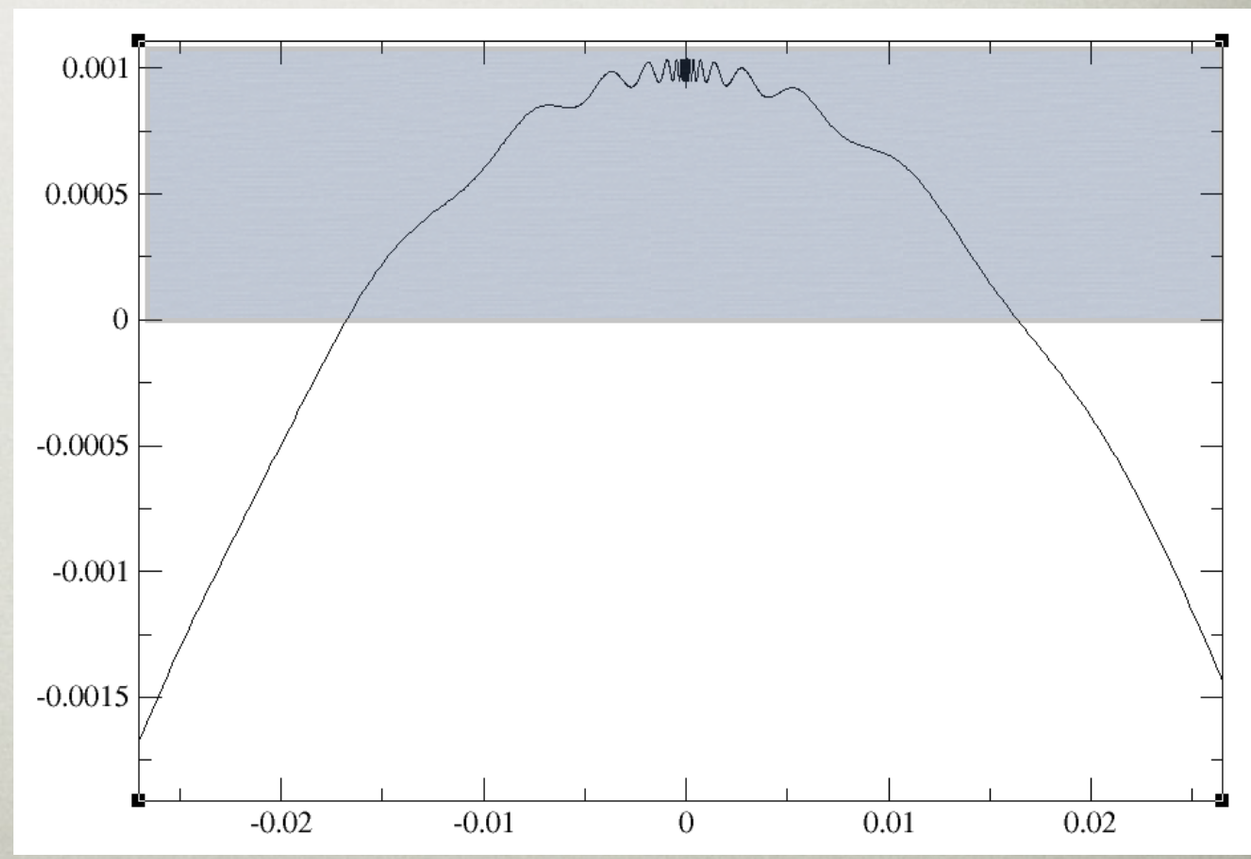
0.001
0.0005
0
-0.0005
-0.001
-0.0015
-0.02
-0.01
0
0.01
0.02

Z-AVERAGING

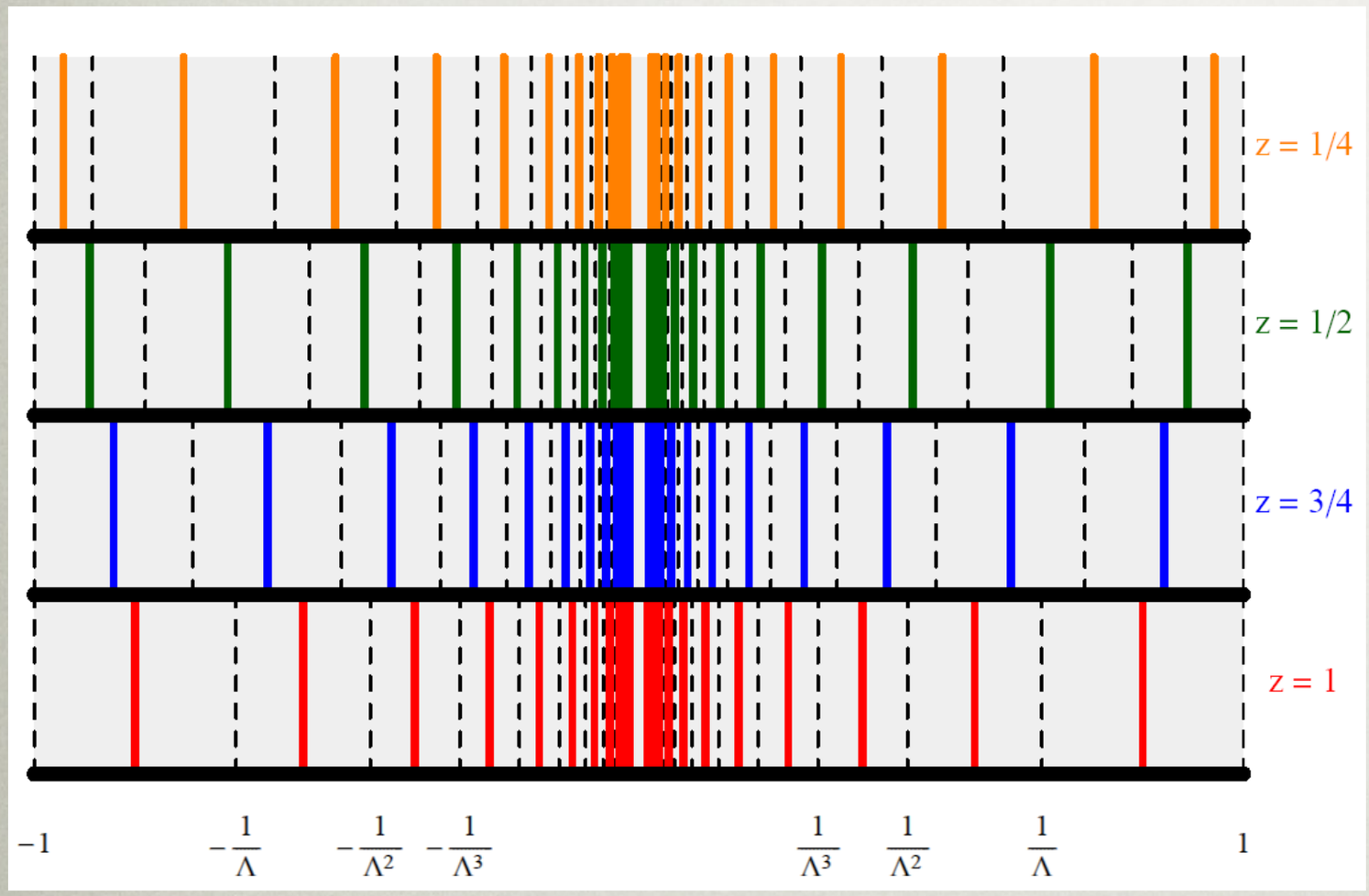

$$\epsilon_1^z = D$$

$$\epsilon_j^z = D\Lambda^{2-j-z}$$

$$z \in (0:1]$$

works best for $N_z=2^N$

similar to *twist averaging* over different boundary conditions in finite clusters to reduce the finite-size effects (better k-space sampling)

Frota, Oliveira, PRB 33, 7871 (1986)
Oliveira, Oliveira, PRB 49, 11986 (1994)

```
#!/usr/bin/env looper
#PRELUDE: $Nz=4;
#AUTOLOOP: ${NRGPREFIX} nrginit ; ${NRGPREFIX} nrgrun
#OVERWRITE

[extra]
U=0.01
Gamma=0.001
delta=0

[param]
symtype=QS
discretization=Z
@$z = 1/$Nz; $z <= 1; $z += 1/$Nz
z=$z

Lambda=2
Tmin=1e-10
keepenergy=10
keep=5000

model=SIAM
```

```
#!/bin/bash
FN=spec_FDM_dens_A_d-A_d.dat
Nz=`getNz`
${NRGPREFIX} intavg ${FN} ${Nz}
```

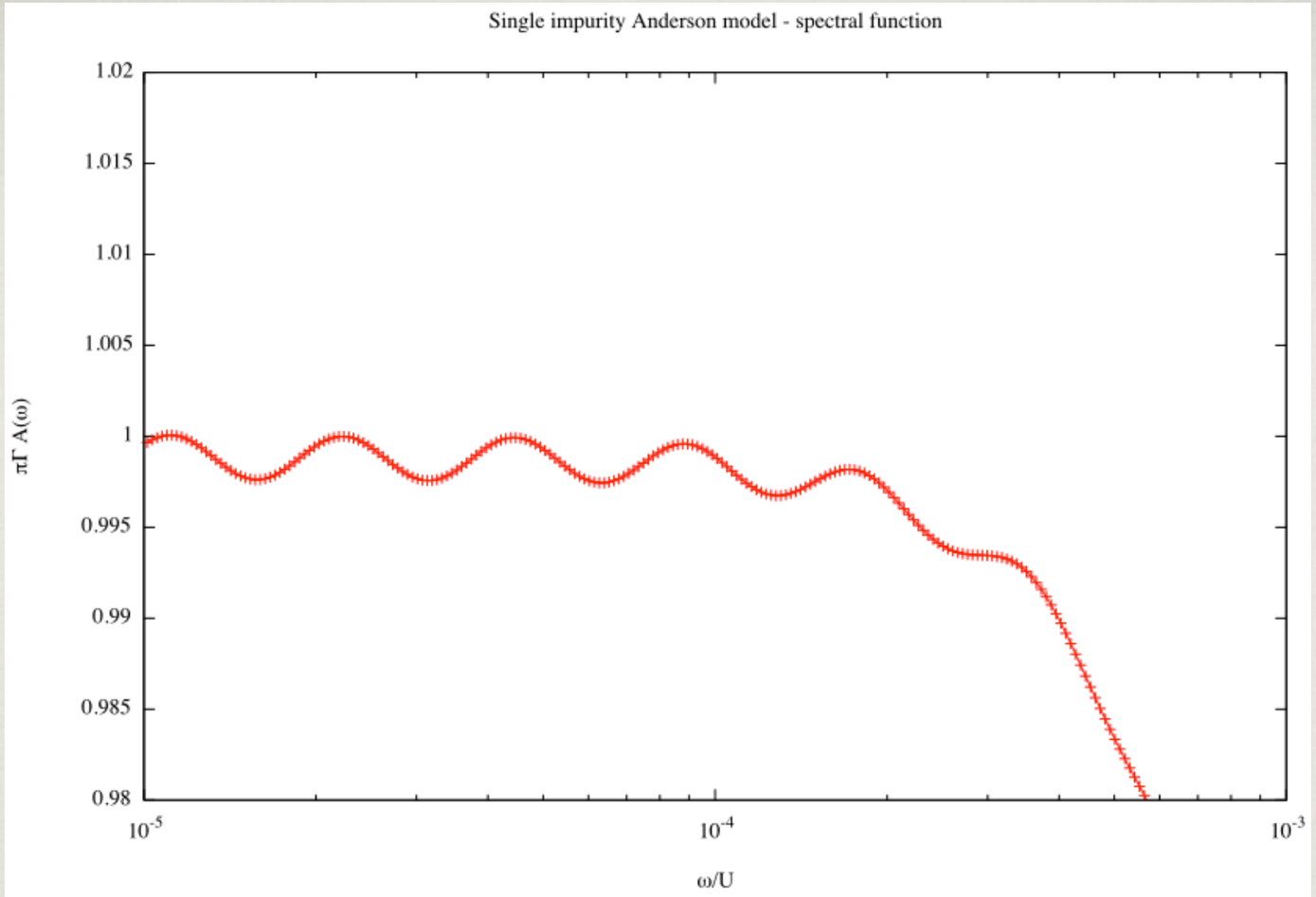
Single impurity Anderson model - spectral function
πΓ A(ω)
1.02
1.015
1.01
1.005
1
0.995
0.99
0.985
0.98
10^-5
10^-4
10^-3
ω/U

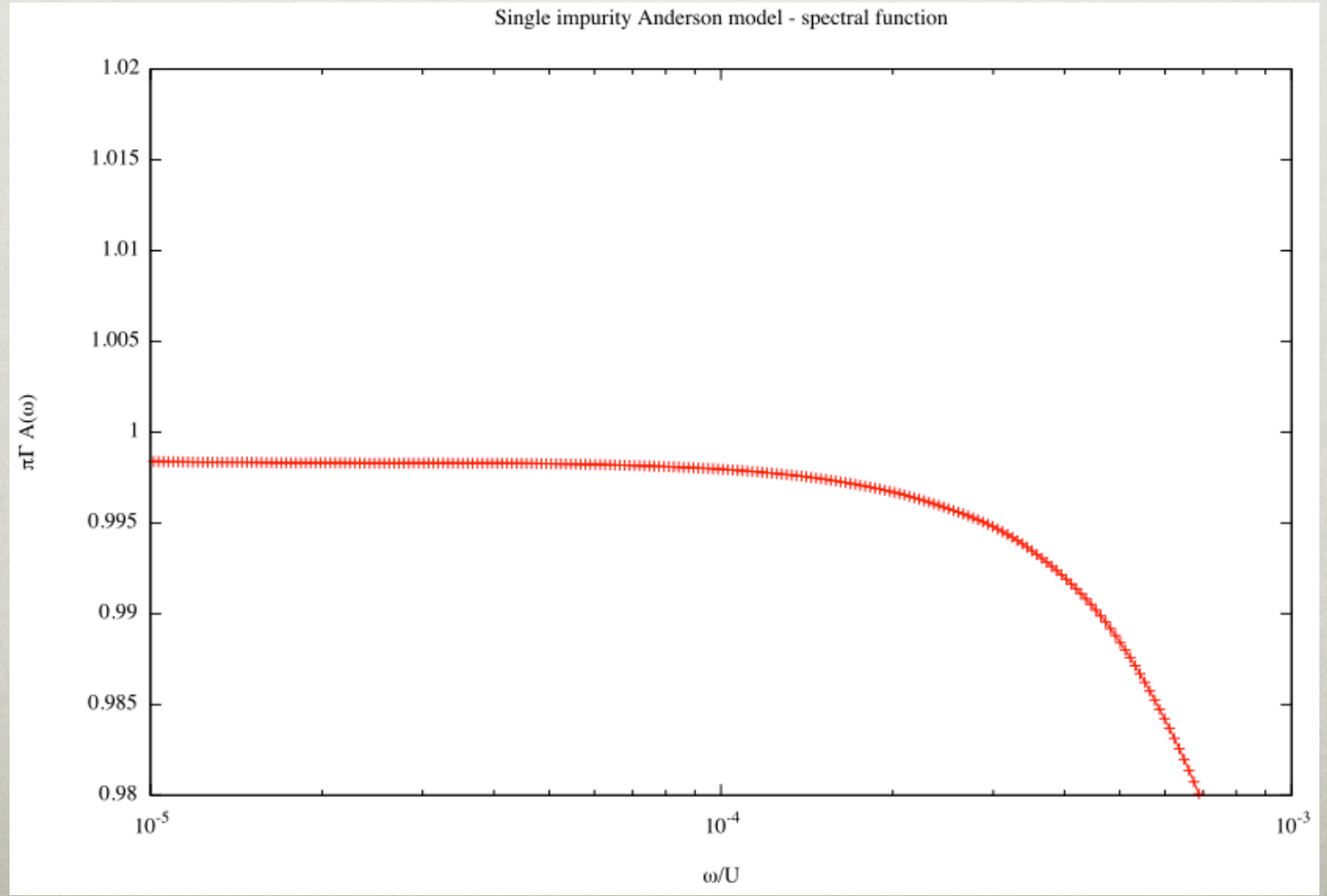
Single impurity Anderson model - spectral function
πΓ A(ω)
1.02
1.015
1.01
1.005
1
0.995
0.99
0.985
0.98
10^-5
10^-4
10^-3
ω/U

Ultimate accuracy limits

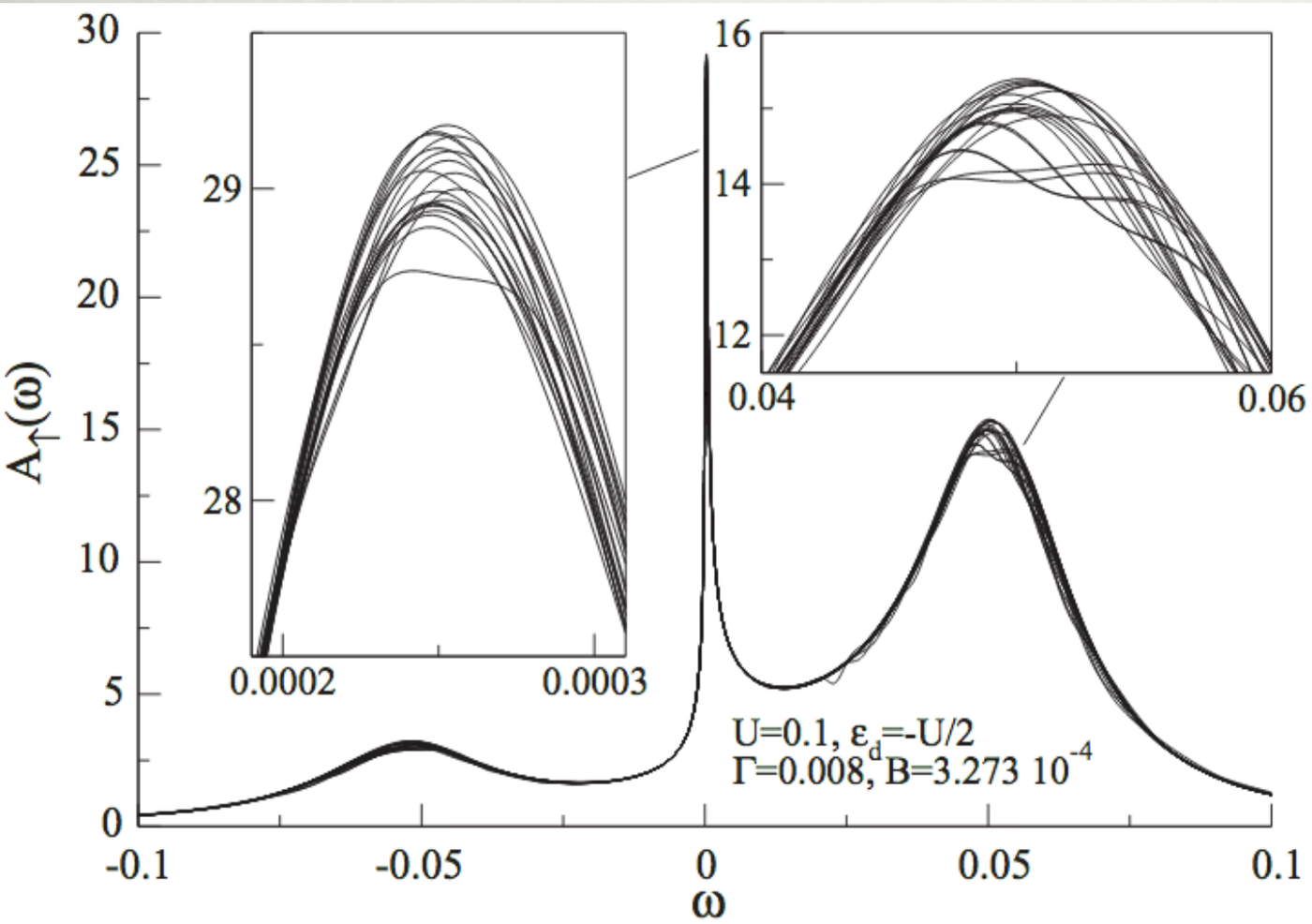

FIG. 1. Spectral function $A_\uparrow(\omega)$ of the Anderson impurity model calculated for a range of N, the number of states kept in the truncation after each NRG iteration step. N ranges from 1800 to 3600 in steps of 100. The Kondo temperature (defined as in Refs. 9 and 10) is $T_K = 6.9 \times 10^{-5}$, and thus $B/T_K = 4.7$.

Zitko, PRB 84, 085142 (2011)

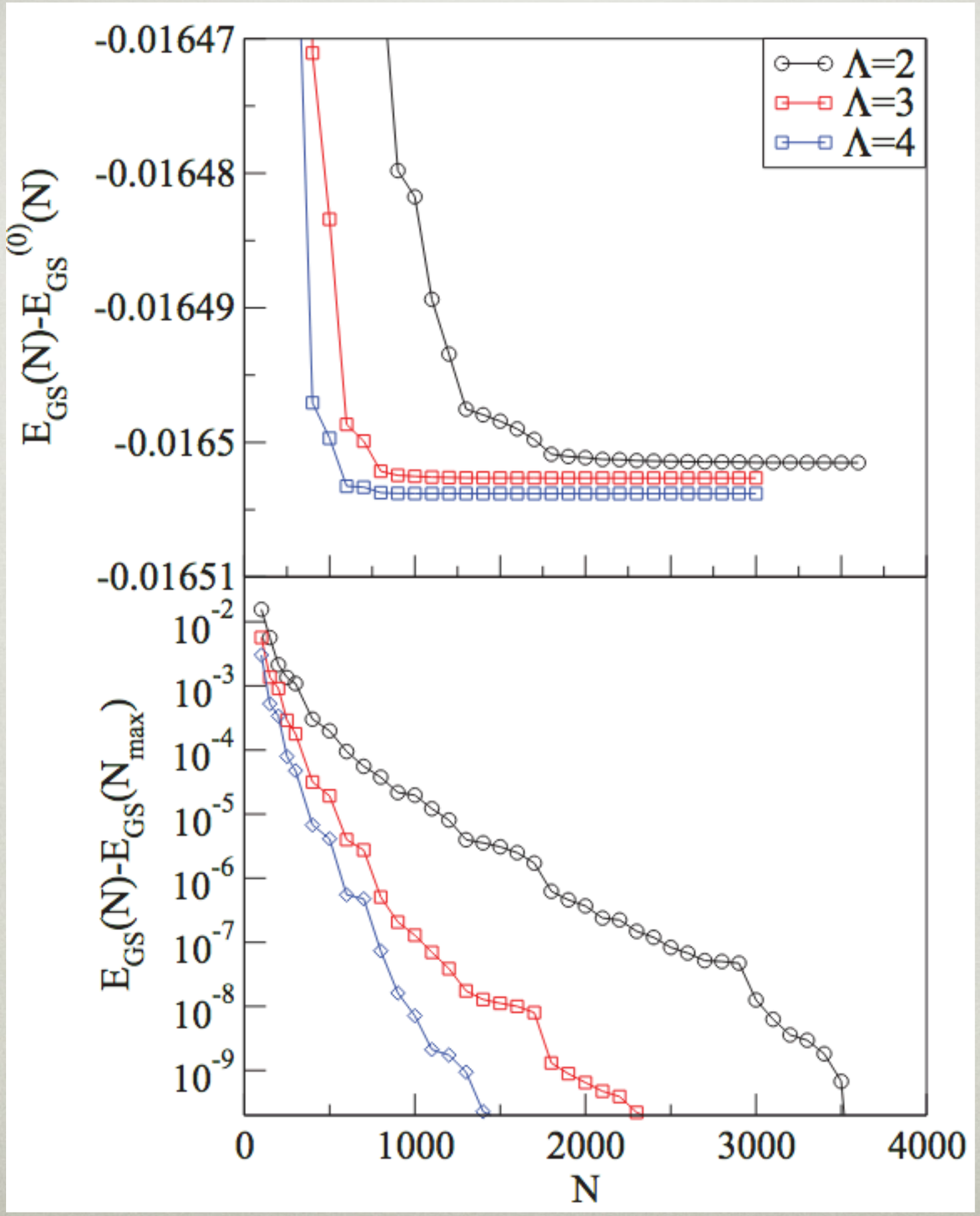
-0.01647
-0.01648
-0.01649
-0.0165
-0.01651
$E_{GS}(N)-E_{GS}^{(0)}(N)$
Λ=2
Λ=3
Λ=4
10^{-2}
10^{-3}
10^{-4}
10^{-5}
10^{-6}
10^{-7}
10^{-8}
10^{-9}
$E_{GS}(N)-E_{GS}(N_{max})$
0
1000
2000
3000
4000
N

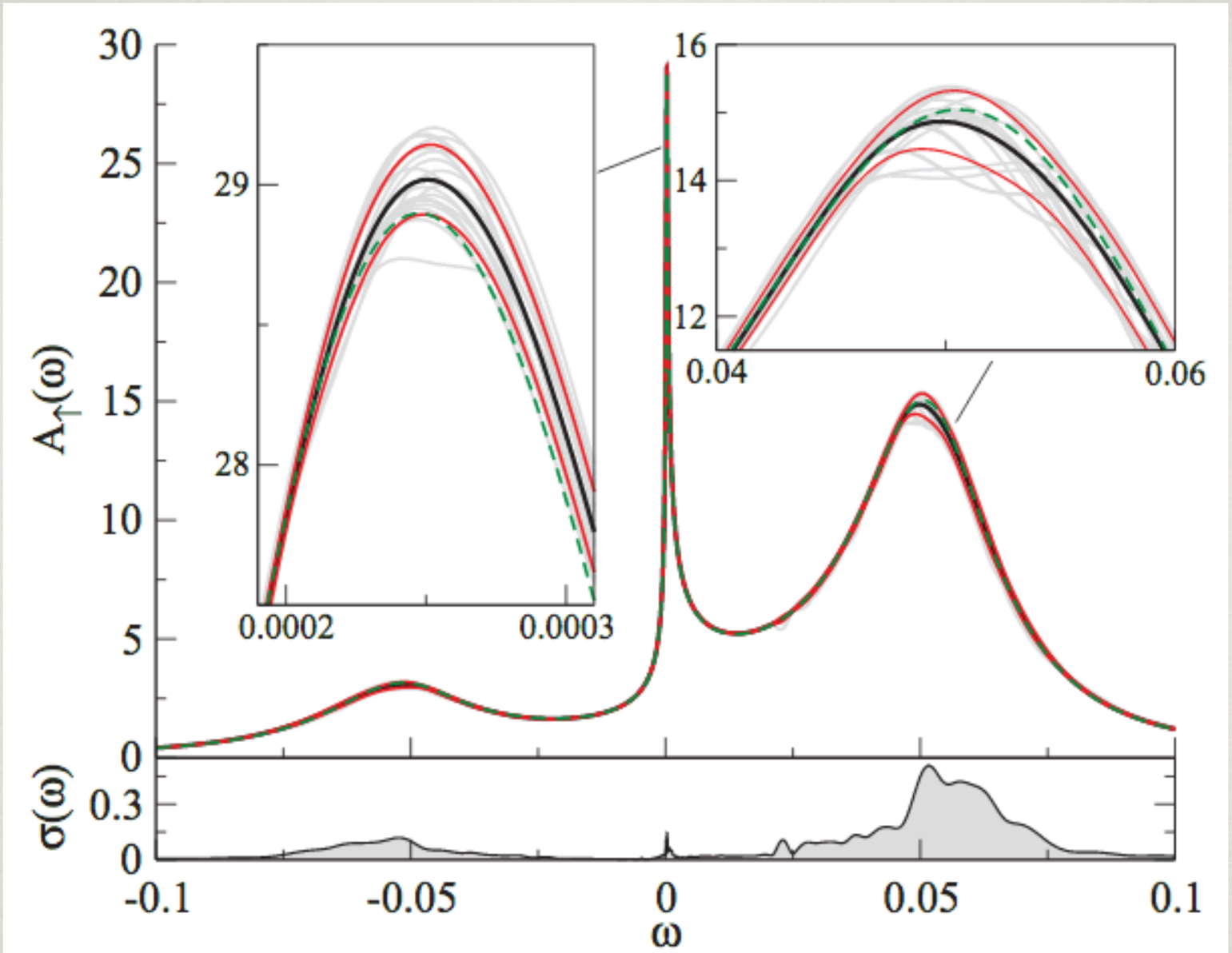

FIG. 3. (Color online) Upper panel: Spectral function calculated by averaging the CFS spectra over all values of N (thick black line) with a confidence interval determined by the standard deviation of the data at each ω (thinner lines; red online). For comparison, the spectral function calculated using the patching approach is also shown (dashed line; green online). The gray lines in the background are the individual CFS spectra from Fig. 1. Lower panel: Standard deviation as a function of frequency.

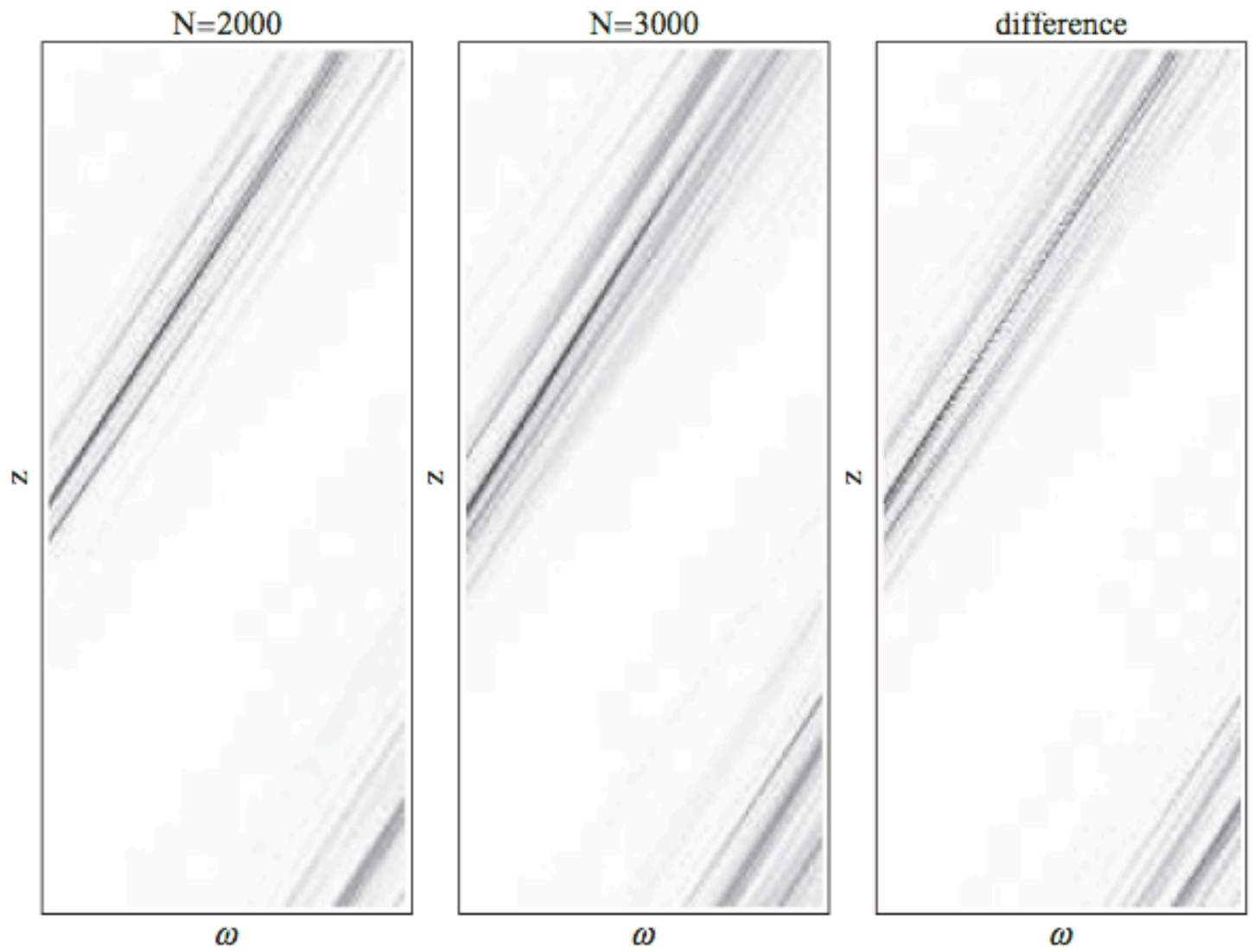

FIG. 5. Raw binned spectral data in the energy range of the Kondo peak for a fine-grained range of z values ($N_z = 256$). These are raw spectral weights of the delta peaks forming the spectral functions which have been binned (using a logarithmic mesh, with 600 bins per decade, the intervals of the binning grid being much narrower than the broadening kernels used to postprocesses these raw results). Left and middle panels show results for $N = 2000$ and $N = 3000$, while the right panel shows the difference between the two. The grayscale ranges are approximately equal in the three plots. In the plots z ranges from 0 to 1 (bottom to top) and ω ranges from 0.0002 to 0.0003 (across the Kondo peak). The model parameters are as in Fig. 1.

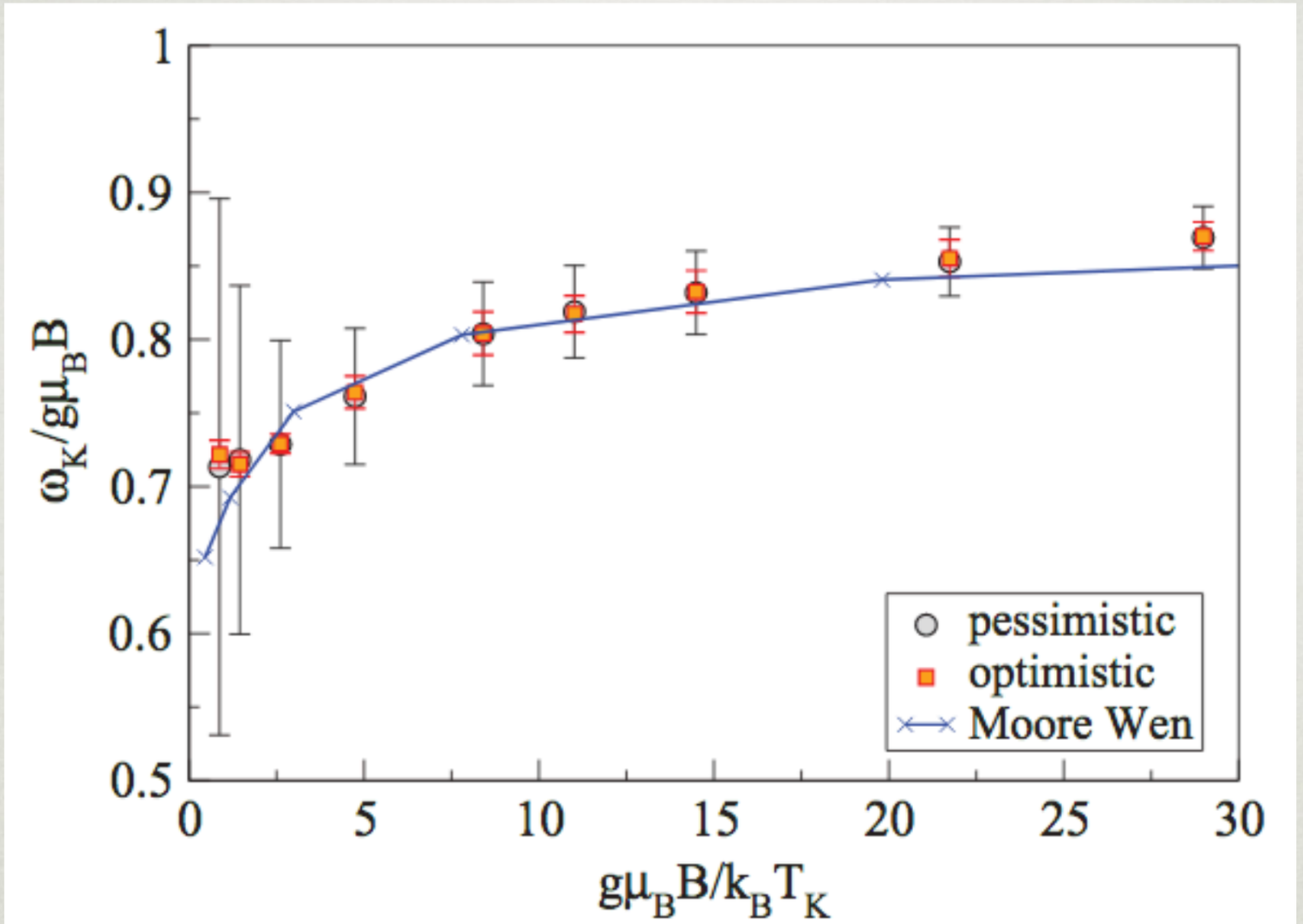

FIG. 8. (Color online) The Kondo resonance splitting as a function of the external magnetic field. The error bars correspond to the "pessimistic" and "optimistic" error estimates. Model parameters are $U = 0.1$, $\epsilon_d = -U/2$, and $\Gamma = 0.008$ in units of half-bandwidth of the (flat) conduction band. The broadening parameter is $\alpha = 0.075$. The data labeled as "Moore Wen" are taken from Fig. 2 in Ref. 37.

Transport in Nanostructures

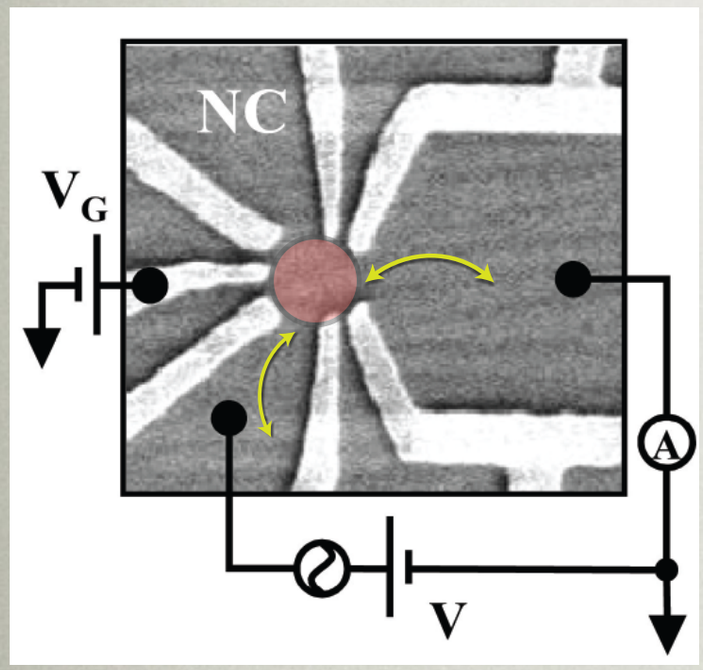

Grobis et al., PRL 100, 246601 (2008)

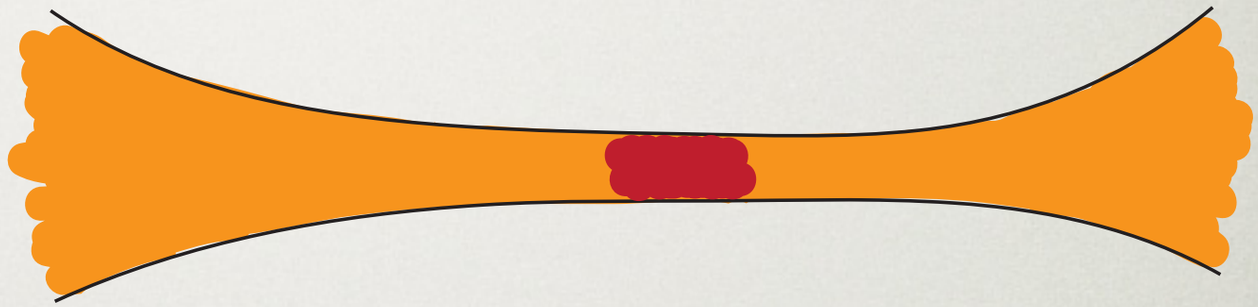

transmission coefficient, T(ϵ)

Landauer formula: $G = \frac{e^2}{h} \sum_\sigma T_\sigma(E_F)$

$$G = \left.\frac{\mathrm{d}I}{\mathrm{d}V}\right|_{V=0}$$

Conductance quantum: $G_0 = \frac{2e^2}{h} = 1/12.906\,\mathrm{k}\Omega$

Conductance calculation using NRG

$$G(T) = G_0 \pi \Gamma \int_{-\infty}^{\infty} \mathrm{d}\omega \left(-\frac{\partial f}{\partial \omega} \right) A(\omega, T)$$

Can be performed without explicitly computing A(ω,T).

Yoshida, Seridonio, Oliveira PRB (2009)

$$G(T) = \mathcal{G}_2 \frac{\beta \pi \Gamma_w}{\mathcal{Z}} \sum_{mn} \frac{|\langle m|c_d|n\rangle|^2}{e^{\beta E_m} + e^{\beta E_n}}$$

$$\mathcal{G}_2 \equiv 2e^2/h$$

07_conductance_SIAM

```
ops=A_d

specgt=A_d-A_d
speci1t=A_d-A_d
speci2t=A_d-A_d
gtp=0.7
```

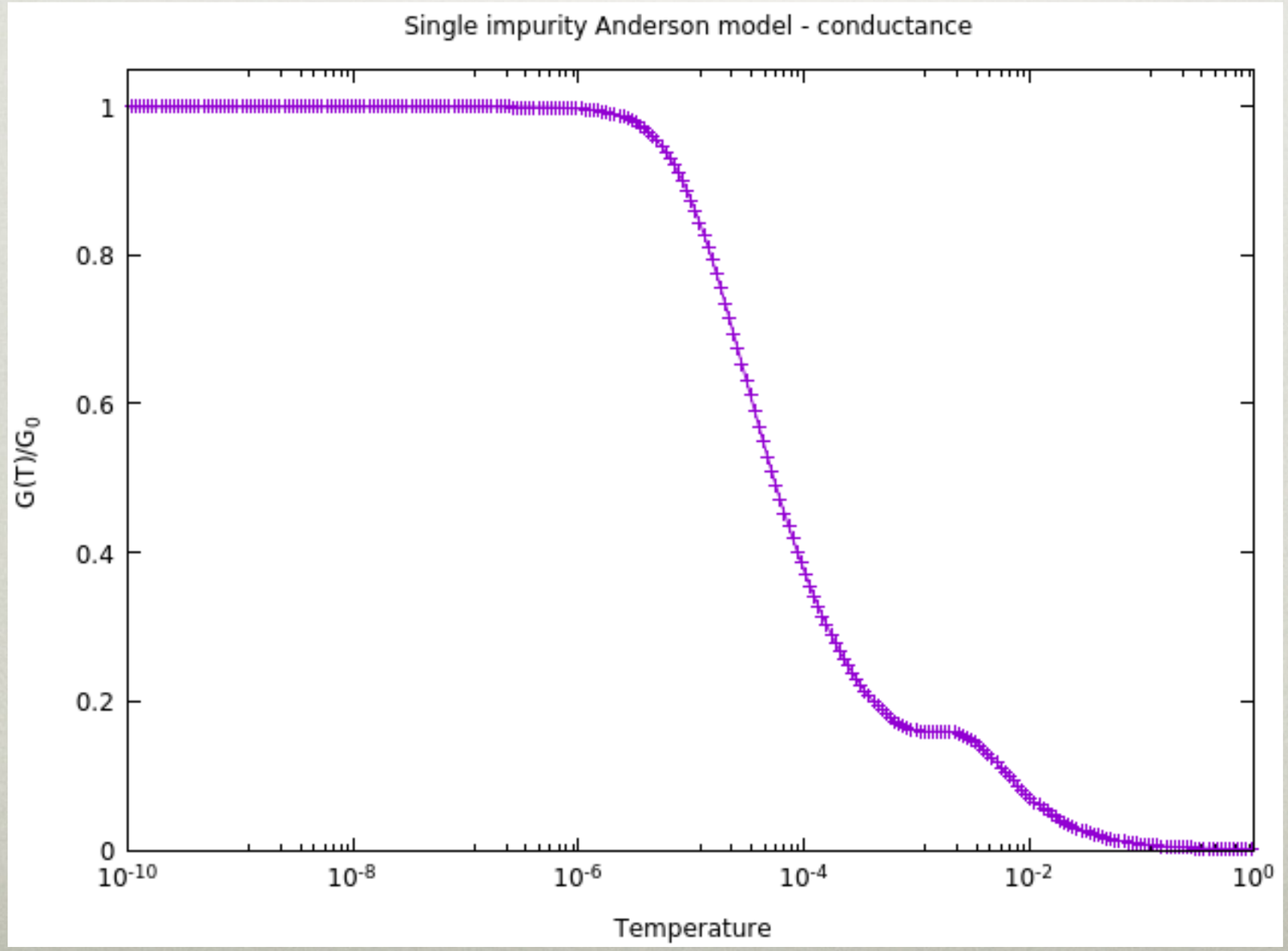

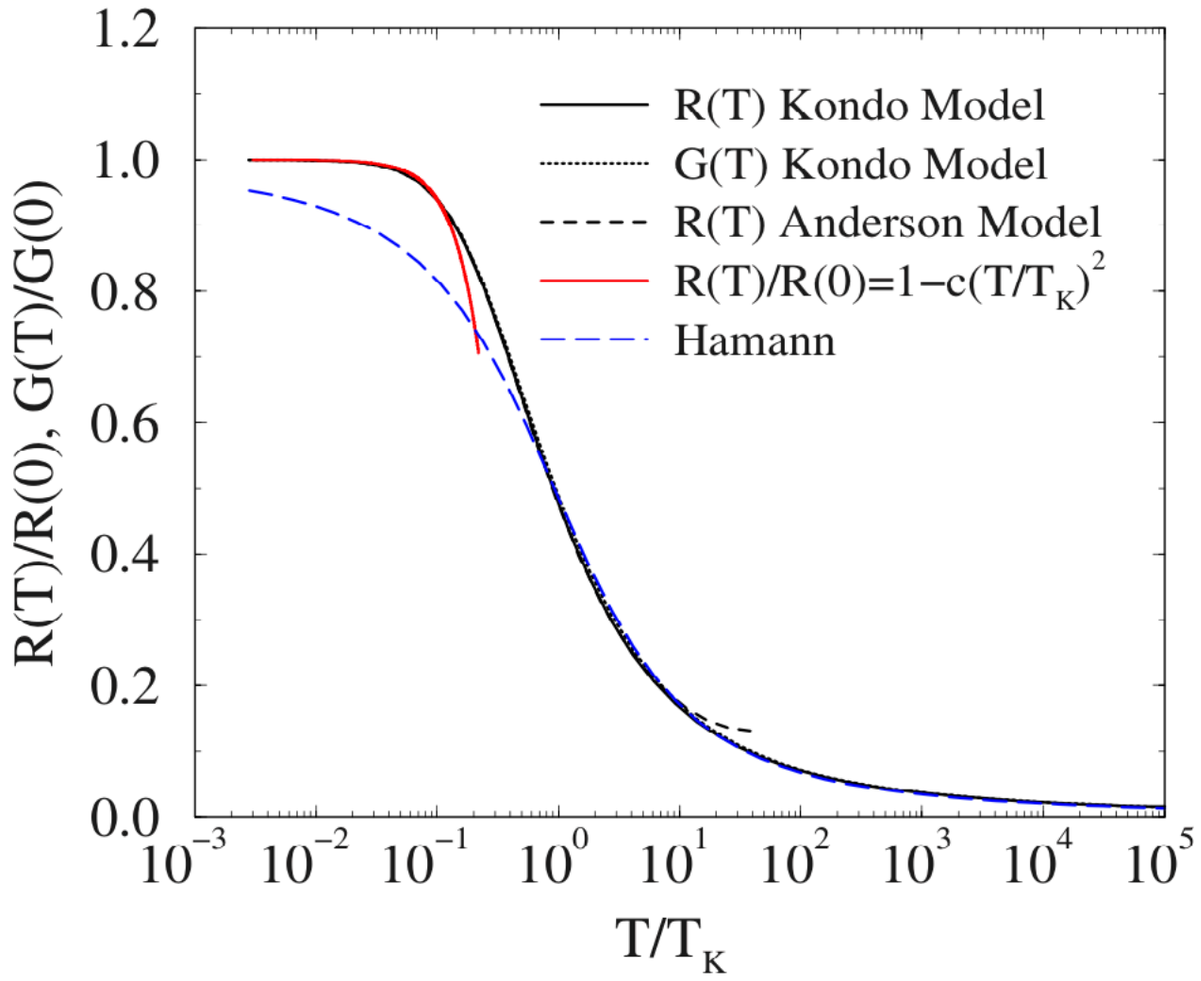

FIG. 10. (Color online) Scaled resistivity and conductance of the $S=1/2$ Kondo model. For comparison the resistivity of the symmetric Anderson model for $U/\pi\Delta=4$ is also shown (Costi and Hewson, 1993) and seen to be identical to that for the Kondo model, up to nonuniversal corrections arising from charge fluctuations at higher temperatures (for $U/\pi\Delta=4$ these corrections occur for $T>10T_K$). Adapted from Costi, 2000.

Figure 10 compares the scaled resistivity $R(T)/R(0)$ for the Kondo and Anderson models with the scaled conductance $G(T)/G(0)$ for the Kondo model. The conductance and resistivity are seen to be almost identical universal functions of T/T_K. At finite magnetic field, the two quantities deviate from each other in the region $T \approx B$ (Costi, 2000). The NRG results can be compared to

$\approx B$ (Costi, 2000). The NRG results can be compared to analytic results at low and high temperatures. The resistivity of the Anderson model in the low-temperature Fermi-liquid regime is given by the result of Nozières (1974),

$$R(T)/R(0) = G(T)/G(0) = 1 - c\left(\frac{T}{T_K}\right)^2, \quad T \ll T_K, \tag{81}$$

where $c = \pi^4/16 = 6.088$ and T_K is the low-temperature Kondo scale defined from the static spin susceptibility via

$$\chi(T=0) = (g\mu_B)^2/4k_B T_K. \tag{82}$$

At high temperatures $T > T_K$, Hamann used the Nagaoka-Suhl approximation (Hewson, 1993a) to obtain for the resistivity of the Kondo model

$$R(T)/R(0) = \frac{1}{2}\left(1 - \frac{\ln(T/T_{\mathrm{KH}})}{[\ln(T/T_{\mathrm{KH}})^2 + \pi^2 S(S+1)]^{1/2}}\right),$$

where S is the impurity spin and T_{KH} is a Kondo scale defined by

$$R(T = T_{\mathrm{KH}}) = R(0)/2. \tag{84}$$

Micklitz *et al.* (2006) found numerically that $T_{\mathrm{KH}} \approx 0.91 T_{\mathrm{K}}$. We see from Fig. 10 that the NRG result for

Standard Kondo effect

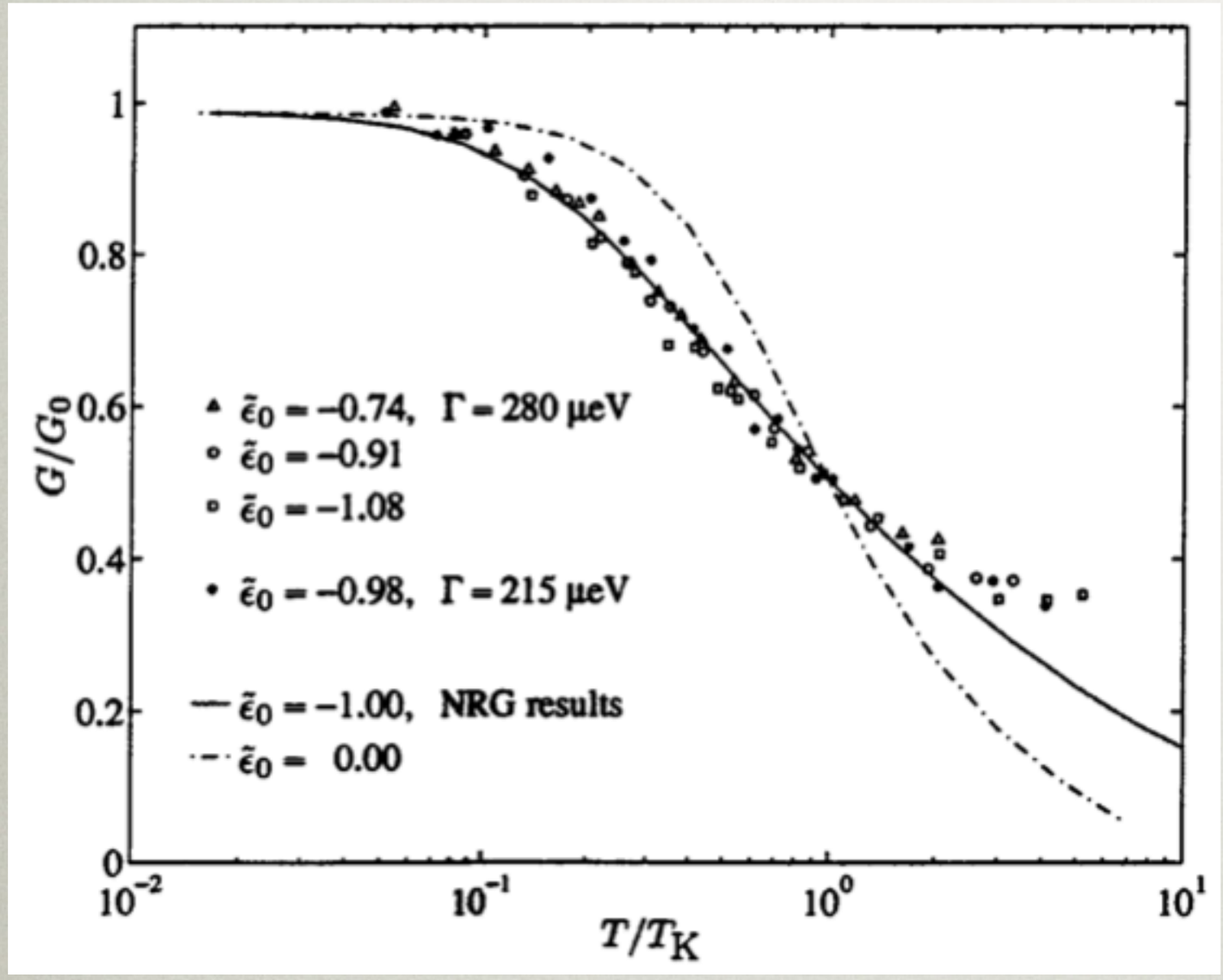

$$G(T_K) = G_0/2$$

$$G(T) = G_0 \left[1 + (2^{1/s} - 1)(T/T_K)\right]^{-s}$$

s=0.22

Goldhaber-Gordon et al., Phys. Rev. Lett. 81, 5225 (1998)

Underscreened Kondo Effect

C_{60} molecule

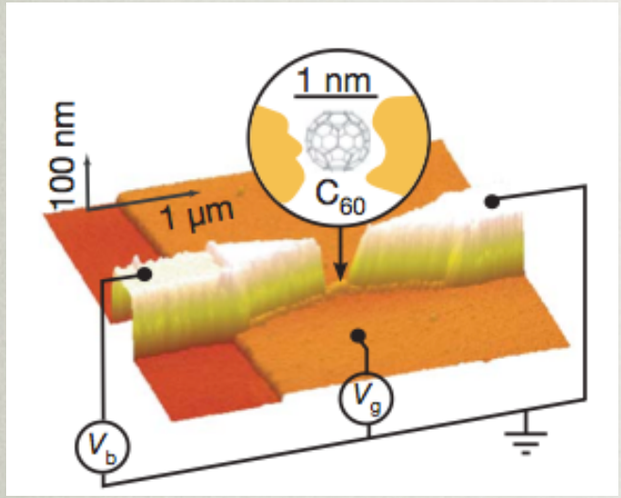

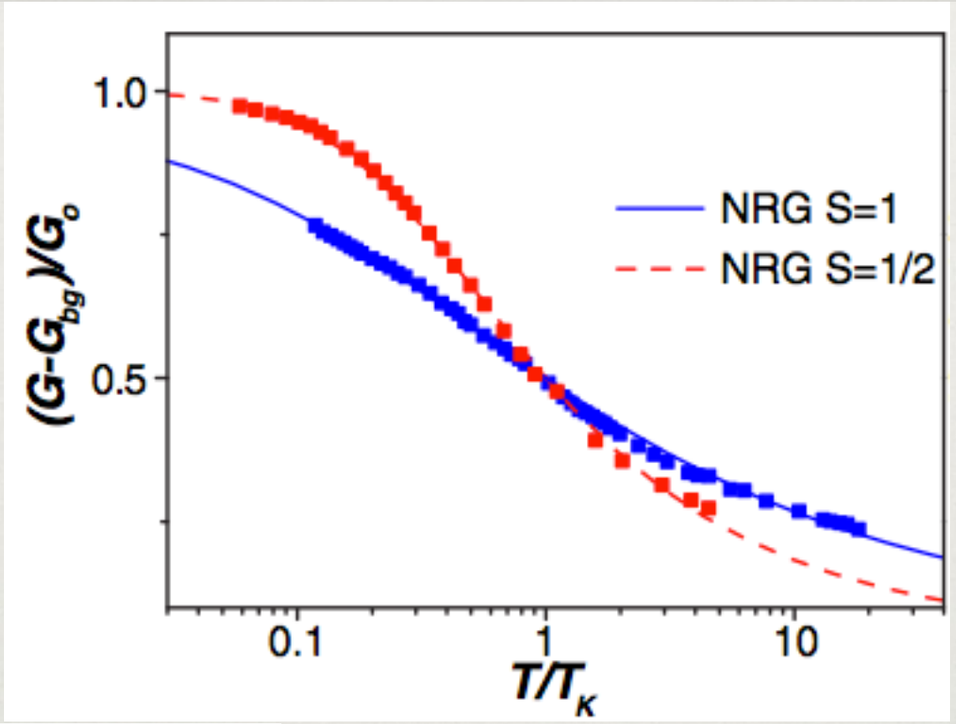

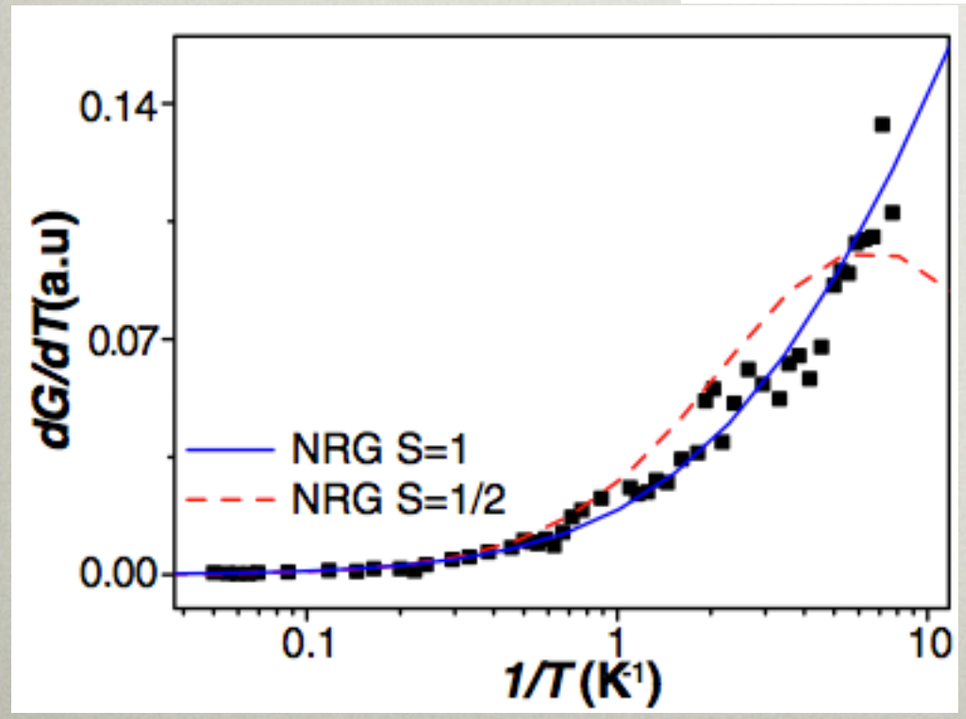

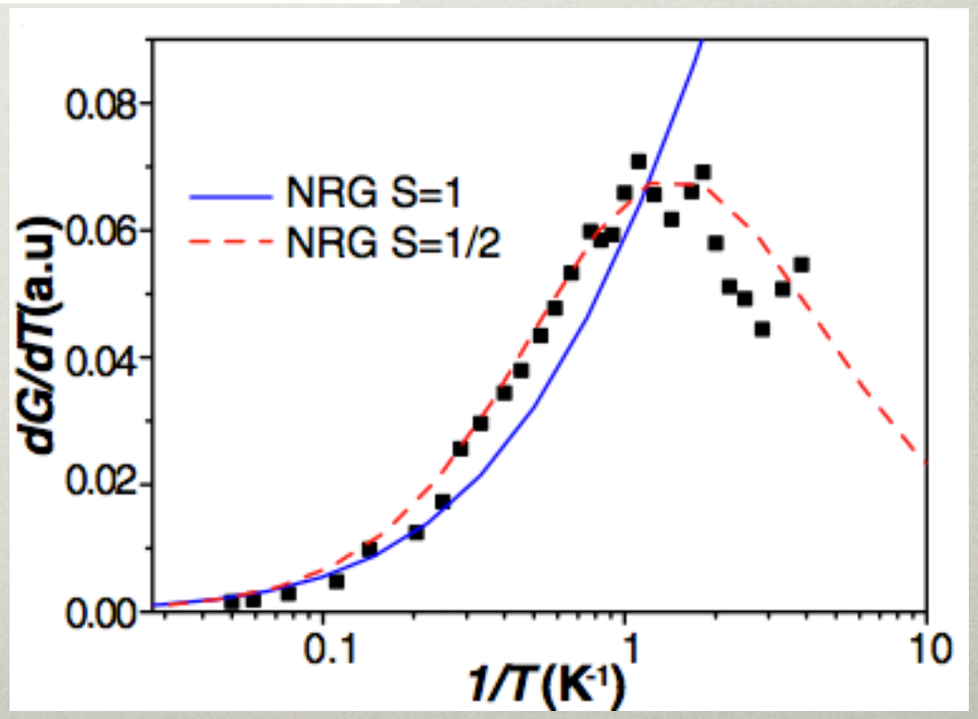

N. Roch, S. Florens, T. A. Costi, W. Wernsdorfer, F. Balestro, PRL 103, 197202 (2009)

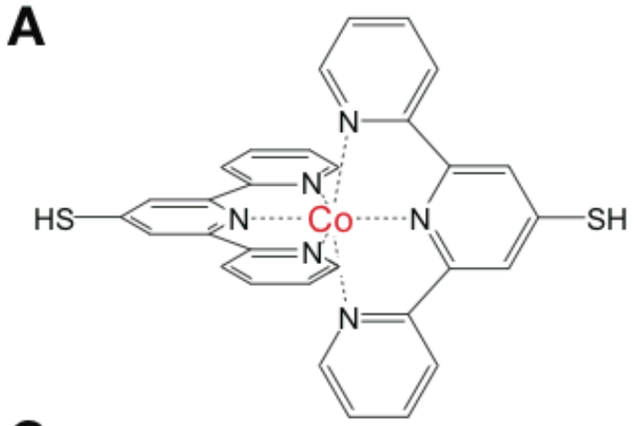

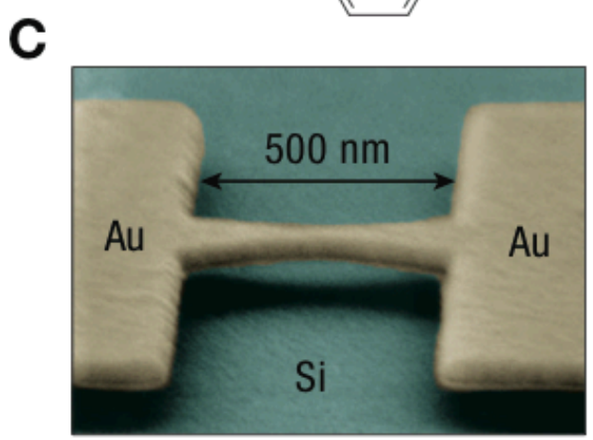

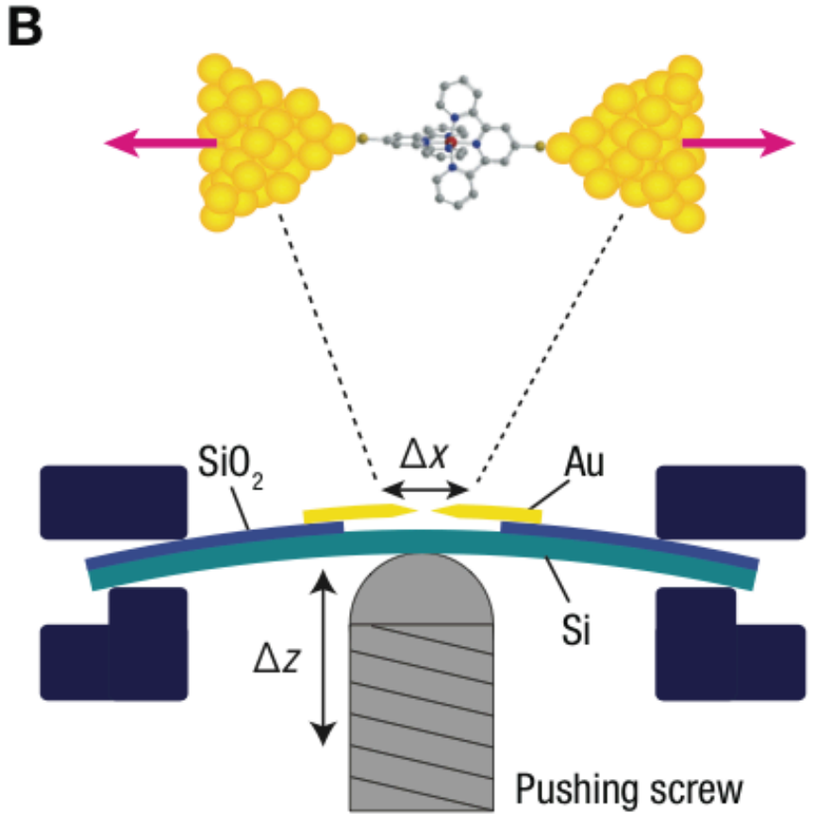

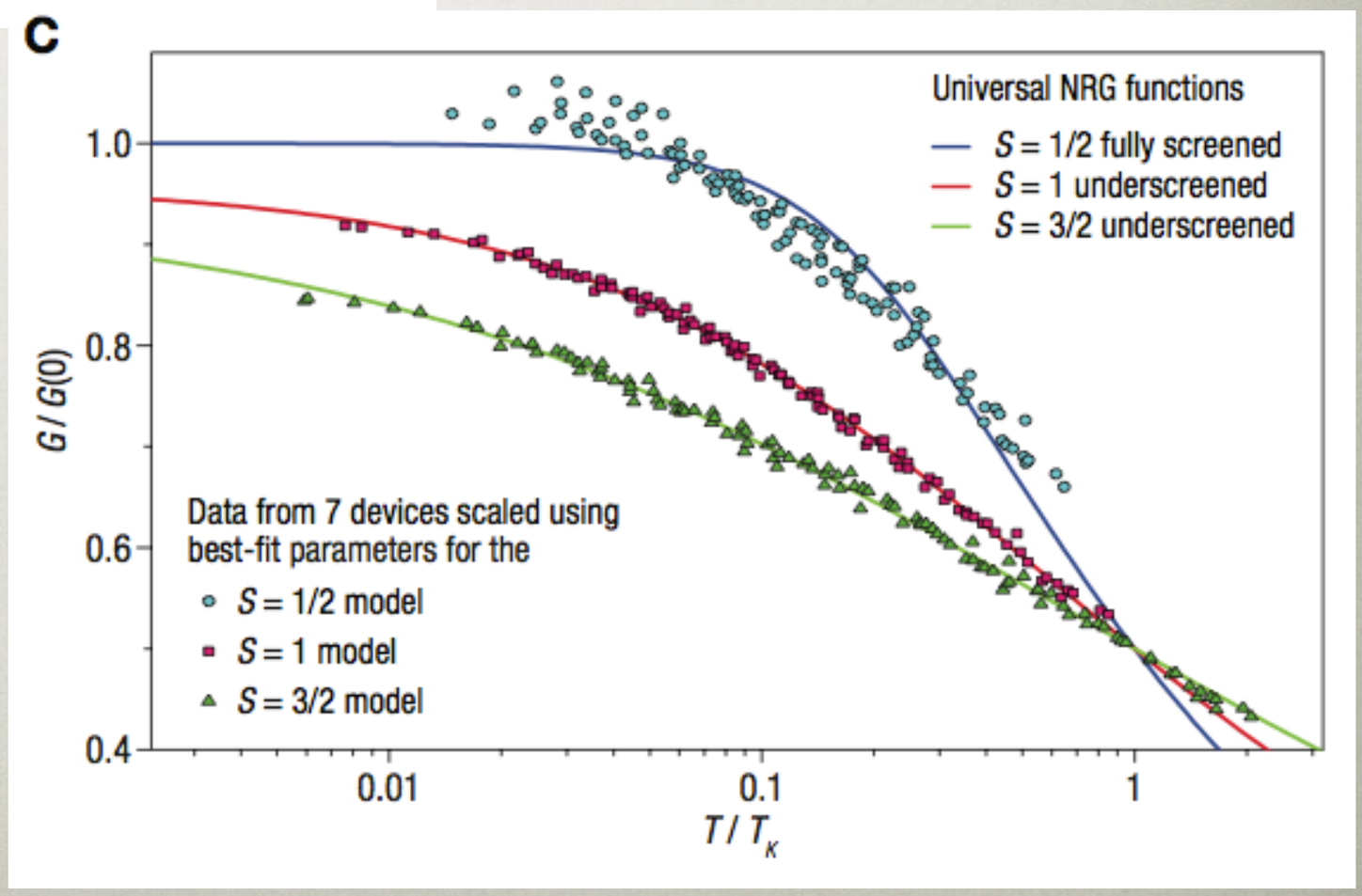

J. J. Parks, A. R. Champagne, T. A. Costi, W. W. Shum, A. N. Pasupathy, E. Neuscamman, S. Flores-Torres, P. S. Cornaglia, A. A. Aligia, C. A. Balseiro, G. K.-L. Chan, H. A. Abruna, and D. C. Ralph. Science 328, 1370 (2010)

Two-Channel Kondo effect

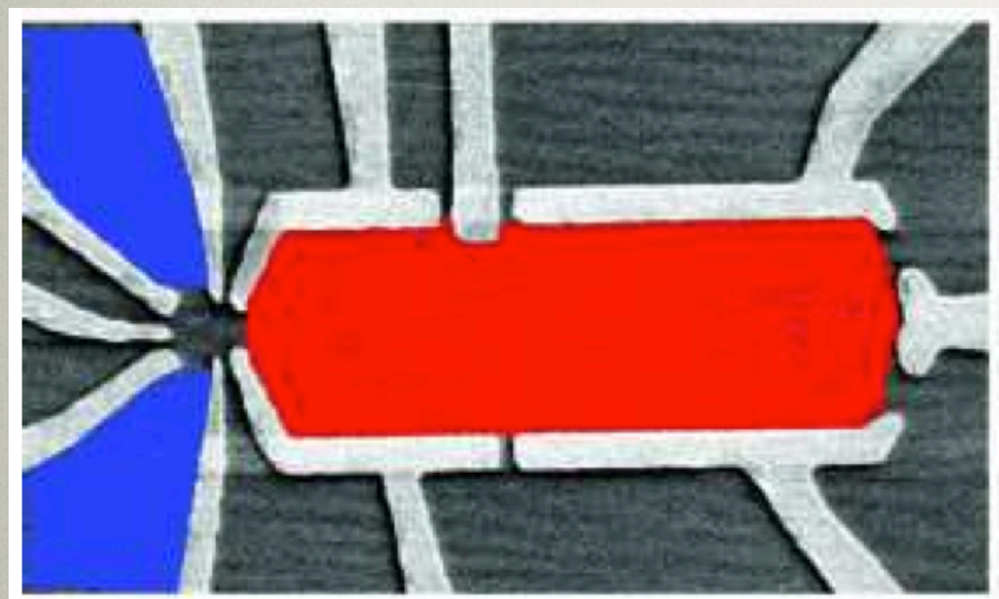

$$\frac{g(0,T) - g(V_{\mathrm{sd}},T)}{T^{0.5}} \propto Y\left(\frac{eV_{\mathrm{ds}}}{k_B T}\right)$$

$$Y(x) \approx \begin{cases} \frac{3}{\pi}\sqrt{x} - 1 & \text{for } x \gg 1 \\ cx^2 & \text{for } x \ll 1 \end{cases}$$

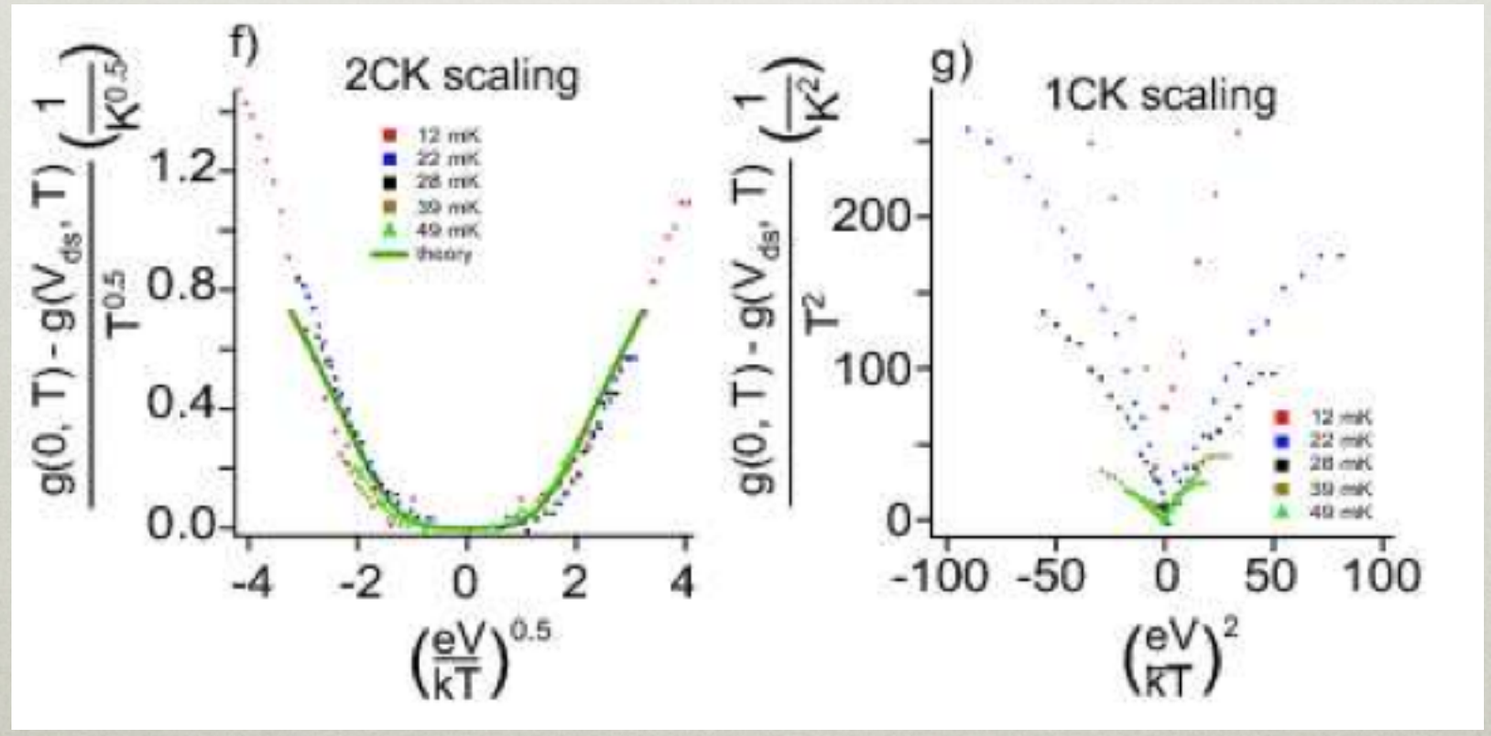

R. M. Potok, I. G. Rau, Hadas Shtrikman, Yuval Oreg, and D. Goldhaber-Gordon, Nature 446, 167 (2007)